# nature communications



**Article** 

https://doi.org/10.1038/s41467-025-64169-5

# Genome-wide CRISPR Screen Identifies Sec31A as a Key Regulator of Alpha Cell Survival

Received: 7 October 2023

Accepted: 9 September 2025

Published online: 15 October 2025

Check for updates

Kimitaka Shibue<sup>1,2</sup>, Sevim Kahraman <sup>1</sup>, Jorge Ivan Castillo-Quan <sup>1</sup>, Dario F. De Jesus<sup>1</sup>, Jiang Hu<sup>1</sup>, Hiroyuki Morita<sup>2</sup>, T. Keith Blackwell <sup>1,3,4</sup>, Peng Yi <sup>1</sup> & Rohit N. Kulkarni <sup>1,3</sup> ⊠

Glucagon, secreted by pancreatic alpha cells, is essential for maintaining normal blood glucose levels. In type 1 and advanced type 2 diabetes, alpha cells often fail to respond to low glucose, yet the mechanisms underlying their stress resistance remain unclear. To investigate this, we performed a genomewide CRISPR screen and identify *Sec31A*, a gene involved in transporting proteins from the endoplasmic reticulum (ER), as a key regulator of alpha cell survival under stress. We show that loss of *Sec31A* enhances survival in stressed mouse alpha cells and in *C. elegans*. In human islets, *SEC31A* expression increases in alpha cells under inflammatory stress, and this upregulation is reversed by reducing ER stress. Functional studies in lab-grown human islet clusters reveal distinct responses in alpha versus beta cells following *Sec31A* suppression. We also find that *Sec31A* interacts with the insulin receptor, suggesting a link between stress adaptation and insulin signaling in alpha cells.

Diabetes is a chronic disease characterized by unstable glycemic control due to disturbed insulin and/or glucagon secretion patterns<sup>1</sup>. Preventing severe hypoglycemia, which, if untreated, can lead to seizures, coma, or irreversible brain damage, remains a challenge in diabetes management<sup>2</sup>. Beyond its physical effects, the anxiety of nocturnal hypoglycemic episodes can also induce psychological stress in patients and their families<sup>3</sup>.

In the context of type 1 diabetes (T1D) and severe type 2 diabetes (T2D), where insulin secretion is absent or its bioactivity is significantly reduced, glucagon secretion by alpha cells becomes a key regulatory factor for glucose homeostasis<sup>4</sup>. However, in T1D and advanced T2D, the glucagon response to hypoglycemia is often impaired<sup>5-8</sup> – an aspect of disease pathology that is poorly understood.

Endoplasmic reticulum (ER) stress, a condition characterized by an overload of unfolded or misfolded proteins, is a pivotal factor influencing the survival and function of islet cells in diabetes<sup>9</sup>. Cells can typically mitigate mild ER stress through an adaptive unfolded protein response (UPR). However, when external stressors exceed this adaptive capacity, susceptibility to apoptosis increases<sup>10</sup>. An interesting study using single-cell RNA sequencing (scRNA-seq) of T1D alpha cells has revealed changes in the expression of potassium and sodium ion channels, vesicle trafficking proteins, and molecules involved in cAMP signaling<sup>11</sup>. These modifications suggest alterations in the electrical activity of alpha cells in T1D and compromised glucagon secretion<sup>11</sup>. To understand how stress affects the function and survival of each islet cell type, it is essential to explore the ER stress-resistance mechanisms specific to each cell type. Alpha-cells are perceived to be relatively more resistant to stress than beta-cells, as evidenced by their persistence in T1D<sup>12</sup>, and maintenance of alpha-cell mass in T2D in contrast to loss of beta-cells<sup>13</sup>.

Studies indicate that in T1D, alpha cells show an increased expression of genes associated with the unfolded protein response<sup>11</sup>, pointing to a unique capacity of these cells to effectively manage ER stress compared to beta cells, which are more susceptible to

<sup>1</sup>Islet Cell and Regenerative Biology, Joslin Diabetes Center, Department of Medicine, Beth Israel Deaconess Medical Center, Harvard Stem Cell Institute, Harvard Medical School, Boston, MA, USA. <sup>2</sup>Medical Research Institute, KITANO HOSPITAL, Osaka, Japan. <sup>3</sup>Harvard Stem Cell Institute, Boston, MA, USA. <sup>4</sup>Deceased: This work is dedicated to the memory of T. Keith Blackwell, whose contributions were instrumental to the completion of this study. —e-mail: Rohit.Kulkarni@joslin.harvard.edu destruction under similar conditions. In patients with T2D, alpha cell mass is either unchanged or increased<sup>13-16</sup> despite chronic exposure to metabolic stressors such as high glucose and/or high free fatty acids. which have deleterious effects on beta cell mass<sup>17-20</sup>. It is not fully explored whether the differential responses observed in the two islet cell types under similar stress conditions are due to the relatively high secretory demand of insulin in beta cells21. This resilience is further supported by gene expression patterns; for example, the key antiapoptotic gene BCL2L1 is more highly expressed in alpha-cells compared to beta-cells<sup>22,23</sup>. In addition, genes associated with ER stress are differentially expressed, with the pro-apoptotic gene CHOP found at higher levels in beta-cells<sup>24</sup>. The expression of oligoadenylate synthetase (OAS) genes has also been recently implicated as being differentially regulated by redox status in the two cell types<sup>25</sup>. It is worth noting that impaired glucagon responsiveness to hypoglycemia was improved by correction of hyperglycemia in an insulin-independent manner in rats, indicating that glucotoxicity itself regulates glucagon secretion<sup>26</sup>. Building on this understanding, by using a genome-wide CRISPR screen in the alphaTC6 cell line, we identified Sec31A as a key component correlated with increased stress resistance. Sec31A is involved in the COPII (Coat Protein Complex II), which is essential for forming transport vesicles from the ER and segregating export cargo, from ER-resident proteins for delivery to the Golgi complex, suggesting its pivotal role in managing ER stress in alpha cells. In addition, evaluating the impact of Sec31A/SEC31A on hormone production in alphaTC6 cells and EndoCβH5 cells, respectively, confirmed the distinct role of Sec31A/SEC31A in regulating ER stress responses and glucagon or insulin production. Treatment of human islets with high glucose and cytokines, as observed by immunohistochemistry (IHC), revealed that SEC31A is expressed in both alpha and beta cells. However, we observed different basal expression levels and responses to cytokine treatment between the cell types. Further investigation revealed a functional link between Sec31A and the insulin signaling pathway in alphaTC6 cells. Taken together this research suggests that targeting Sec31A-dependent pathways offer new therapeutic avenues to protect alpha cells from metabolic stress and better regulate glucagon secretion to improve outcomes in patients with diabetes.

### Results

# Selection of a stress-resistant cell population after TG treatment

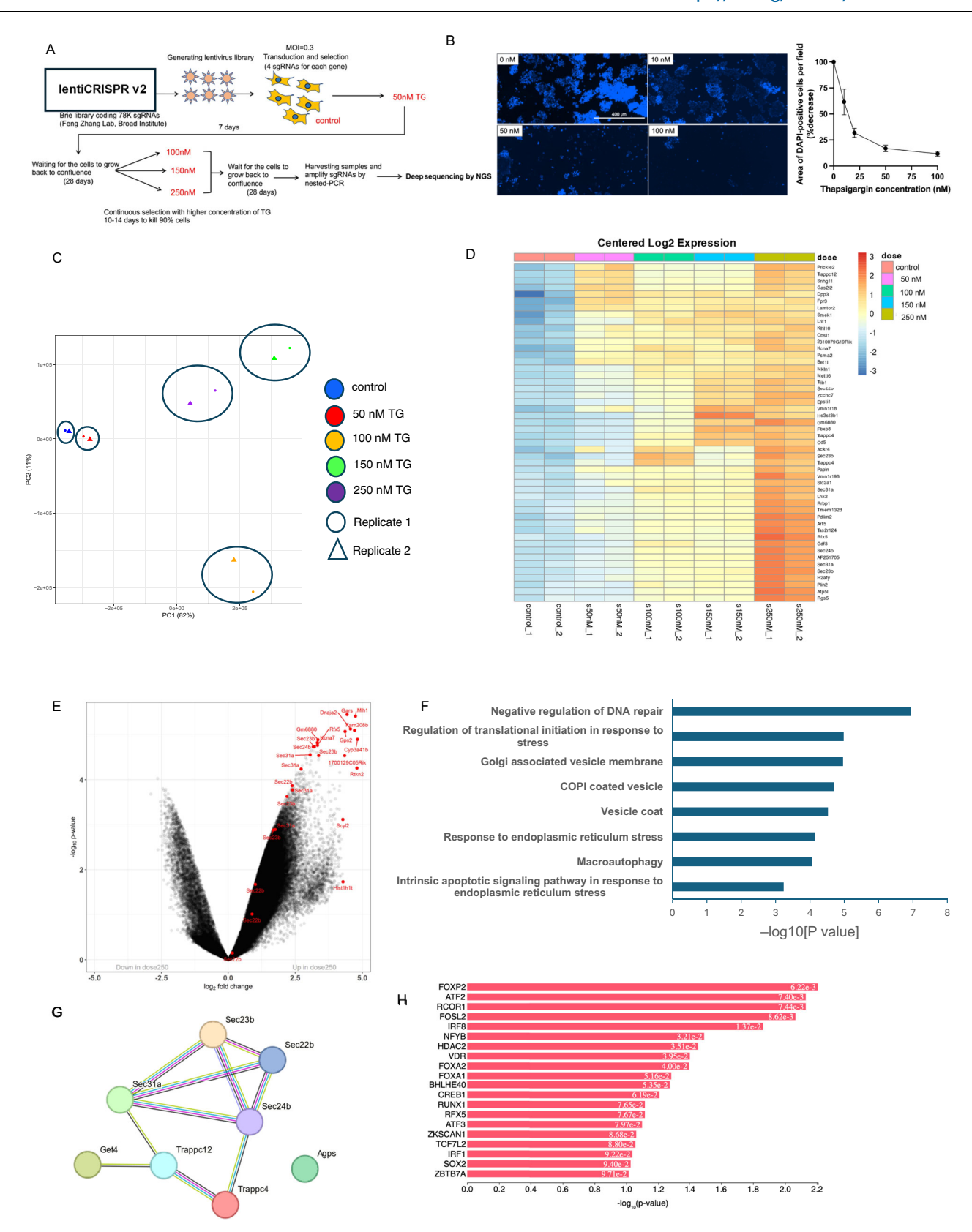
To identify genes responsible for stress resistance in alpha cells, we employed an unbiased genome-wide CRISPR screen<sup>27-29</sup> in a mouse alpha cell line (alphaTC6) using the Brie CRISPR library targeting 19,674 genes with 78,637 sgRNAs<sup>30</sup> (Fig. 1A). We induced stress by treating the cells with the ER stressor, thapsigargin (TG), at various doses for 7 days and evaluated alpha-cell survival (Fig. 1B). Increasing doses of TG up to 50 nM killed ~75% while 100 nM killed 90% of cells in a week, respectively (Fig. 1B, right panel). Based on these observations, we pretreated the cells with 50 nM of TG prior to screening to eliminate the cells responding to low-intensity stress. Next, to select the cell population that are resistant to high-intensity stress, we expanded the cells that had survived the 50 nM of TG and then treated them with higher doses of TG (100 nM, 150 nM, or 250 nM) (Fig. 1A) for 10-14 days. We then expanded the surviving cell population for about one month and analyzed the sgRNA profile by NGS. PCA analysis demonstrated that the groups clearly separated according to the concentrations of TG (Fig. 1C). In the lentiviral pooled library that we used in this study, ~4 differently designed sgRNAs were included per gene<sup>30</sup>. Therefore, the greater the enrichment of sgRNAs for a single gene, the greater the reliability of enrichment of the gene in the population. Using this paradigm, we analyzed the top 100 enriched genes in all groups (i.e., treatment with TG at 50, 100, 150, or 250 nM) for differently designed sgRNAs that were enriched. Our study revealed that four genes (Sec23B, Sec31A, Trappc4, and Trappc13) were enriched with multiple sgRNAs that were uniquely designed in the group treated with 250 nM TG. In the same manner, three genes (*Sec22B, Sec23B, and Trappc12*) had sgRNAs enriched in the group treated with 150 nM TG, while only one gene (*Trappc13*) had enriched sgRNA in the group treated with 100 nM TG. Notably, no sgRNA was enriched in the group treated with 50 nM TG (Fig. 1D) (Supplementary Data 1 and 2). Since the group treated with a concentration of 250 nM had the highest number of genes with multiple enriched sgRNAs, we deemed this condition to be the most reliable for identifying candidate genes. Therefore, we pursued further studies to identify the genes that were enriched under this condition.

#### **COPII-related gene deficiency promotes TG resistance**

To identify genes for further study, we compared a control group, which did not receive TG treatment, versus a group treated with 250 nM of TG. We focused on genes that demonstrated stress resistance upon knockdown, as seen in the right portion of the volcano plot in Fig. 1E. Subsequently, we conducted pathway analysis on the top 50 sgRNAs to determine the enriched gene categories. Notably, we discovered a significant enrichment of pathways associated with vesicle transportation, ER-Golgi vesicle-mediated transport, and macroautophagy in the TGtreated groups (Fig. 1F). Furthermore, we analyzed protein-protein interaction networks of these genes and observed a link between coat protein complex II (COPII) genes, such as Sec24B, Sec23B, Sec22B, and Sec31A, belonging to the Sec family and vesicle-transporting genes such as Get4, Trappc4, and Trappc12 (Fig. 1G). Finally, to identify upstream regulatory factors, we performed transcription factor (TF) enrichment analysis of the top genes in the cells receiving 250 nM of TG. Among multiple TFs that were predicted to regulate the genes, FOXP2 has been reported to be responsible for alpha cell replication and function<sup>31</sup> while FOXA2 regulates rodent alpha cell differentiation<sup>32</sup> and the singlevariant of FOXA2 associates with random glucose and fasting glucose in diabetes patients<sup>33,34</sup> (Fig. 1H). We thus identified multiple genes and upstream regulators involved in ER-Golgi and vesicle transportation that are important in inducing resistance to stress, likely due to their absence in alpha cells.

# Lack of Sec31A protects alpha cells from ER stress-induced cell death

During our CRISPR screen, we observed that among the Sec family of genes, Sec31A was singular in that all four of its differently designed sgRNAs were enriched in the group treated with 250 nM TG (Fig. 1G). This observation prompted us to select this gene for further study, hypothesizing that its absence facilitates cell survival in response to ER stress. To confirm that Sec31A is involved in the protection of alpha cells from ER stress-induced apoptosis, we used the CRISPR/ Cas9 system to generate stable Sec31A knockdown (>80% KD of Sec31A protein) in the alphaTC6 cell line (Fig. 2A). Anticipating that Sec31KD cells would withstand a larger concentration of TG, we tested a high-dose TG (1000 nM) treatment, a dosage based on a previous study<sup>35</sup>. Treating the control alpha TC6 cells with high-dose TG induced a significant increase of cleaved caspase-3, a marker of apoptosis, in contrast to a significantly suppressed effect in alphaSec31AKD cells (Fig. 2B). To evaluate whether alphaSec31AKD cells exhibit resistance to long-term ER stress induction, we subjected both control and alphaSec31AKD cells to TG treatment. Fifty hours posttreatment, alphaSec31AKD cells demonstrated improved survival relative to the controls (Fig. 2C). This finding aligns with the observed reduction in the expression of cleaved caspase-3 in alphaSec31AKD cells after TG treatment (Fig. 2B). On the other hand, Sec31A knockdown in mouse beta cell line showed no significant difference in cell survival upon the same TG treatment condition (Supplementary Fig. 1). Finally, we investigated whether the stress-resistant phenotype of alphaSec31AKD cells is also evident when they are exposed to inducers of ER stress other than TG. To this end, we treated control and alphaSec31AKD cells with various concentrations of tunicamycin (inhibits glycosylation of protein) or Brefeldin A (inhibits ER-Golgi



transport). The Western blot analysis confirmed a decrease in expression of cleaved caspase-3 in alphaSec31AKD cells not only by TG but also in response to tunicamycin and Brefeldin A (Fig. 2D). We have also broadened the scope of stressors to evaluate the resilience of alphaSec31A KD cells beyond ER stress inducers. Treatment of the cells with cytokines, palmitate, and H<sub>2</sub>O<sub>2</sub> corroborated the previously

observed trends in stress resistance, similar to those seen with TG treatment. (Fig. 2E, F and H). To further confirm that the observed stress-resistant phenotype of Sec31AKD cells is not due to specific sgRNAs, we conducted a parallel experiment using siRNA to knock down Sec31A. This was followed by TG treatment under identical conditions (Fig. 2G). The results consistently demonstrated that the

**Fig. 1** | **Genome-wide CRISPR screen in alpha cells. A** Overview of the CRISPR screen and subsequent next-generation sequencing (NGS) of enriched guide RNAs (gRNAs). **B** Representative images (left) and dose-dependent survival curve (right) of alphaTC6 cells after treatment with TG (0, 10, 50, and 100 nM) for seven days. Scale bar:  $400 \, \mu m$ . Four biological replicates cultured in independent wells were examined. Data are presented as mean values  $\pm$  SEM. **C** Principal component analysis (PCA) of NGS data. PCA plot showing the variance of each group of samples. **D** Heatmap showing log 2 count per million (cpm) of enriched gRNAs in the survived cells after the treatment with TG (0, 50, 100, 150 and 250 nM). **E** Volcano plot (shown in log2 fold change) of enriched gRNAs in the control cells versus survived cells in 250 nM TG. **F** Gene Ontology Analysis of the top enriched gRNAs in Fig. 1E.

For panels (**E**, **F**), differential expression analysis was performed using limma, applying a one-sided moderated t test to compare drug-treated (250 nM TG) and control groups for genes with increased expression. P-values were adjusted for multiple comparisons using the Benjamini–Hochberg method to control the false discovery rate. **G** Interactive Pathway analysis of the top 50 proteins which gRNAs were enriched in the group of 250 nM TG treatment. **H** Transcription factor (TF) enrichment analysis of the top genes whose gRNAs were enriched in the group receiving 250 nM TG treatment. Enrichment was assessed by a one-sided Fisher's exact test, with p-values adjusted for multiple comparisons using the Benjamini–Hochberg FDR method. Bar heights indicate  $-\log_{10}(\text{raw }P\text{-values})$ . Source data are provided as a Source Data file.

stress-resistant phenotype was independent of the knockdown method used. Consequently, Sec31A deletion confers protection against ER stress induced by agents acting through diverse pathways.

Lastly, we evaluated whether Sec31A's role in stress resistance persists beyond the period of stress induction. Control and alphaSec31AKD cells were treated with TG for a fixed duration, following which TG was removed and the cells were allowed to recover for 24 h. FACS analysis revealed that, after TG removal, control cells maintained significantly elevated levels of early apoptotic cells compared to their baseline, whereas the levels in alphaSec31AKD cells returned to baseline (Q1 in Fig. 2I, J). On the other hand, the number of late apoptotic/ necrotic cells increased in control cells following both the induction and removal of TG, but this TG-responsive increase was not observed in alphaSec31AKD cells (Q2 in Fig. 2I, J). Moreover, throughout the TG induction and removal process, alphaSec31A KD cells consistently exhibited a lower number of both early apoptotic and late apoptotic/ necrotic cells (Fig. 2I, I). These results demonstrate that the survival advantage from Sec31A knockdown persists even after ER stress is removed.

# Sec31A inhibition induces protective organismal response in vivo against ER stress

To examine whether our findings were cell-type specific in vivo and evolutionarily conserved, we considered that a majority, if not all, molecular players of UPR<sup>ER</sup> are identified in the genetically tractable nematode *Caenorhabditis elegans*. Indeed, survival in response to ER stress can be assessed in a timely manner in the nematode<sup>36-38</sup>. *C. elegans* does not possess defined pancreatic alpha or beta cells since its over 40 insulin-like peptides are secreted from neurons, the intestine (gut, liver, and immune functions), and hypodermis<sup>39</sup> and any role of COPII in UPR<sup>ER</sup> likely reflects a global in vivo response.

First, we evaluated whether knockdown of Sec23B or Sec31A orthologs in C. elegans activates the UPR<sup>ER</sup> transcriptional reporter hsp-4p::GFP (GFP fused with the promoter of hsp-4, the ortholog of BiP) in the intestine (Fig. 3A)<sup>40</sup>. While KD of sec-23 (ortholog of mouse and human Sec23B) caused developmental arrest and lethality, RNAi against sec-31 (ortholog of mouse and human Sec31A) did not interfere with development and significantly increased the expression of hsp-4 (Fig. 3B, C). Thus, COPII inhibition induces a mild yet significant UPRER response. Next, we evaluated whether this response would protect worms against ER stress. We first documented that while 24 h tunicamycin treatment induced a marked UPRER stress response, prior KD of sec-23 led to greater hsp-4 transcriptional induction (Fig. 3D, E). Consistent with this, worms in which sec-23 had been KD survived for longer under toxic concentrations of tunicamycin (Fig. 3F). Thus, inhibition of sec-31 elicits a protective response against ER stress. This phenotype is conserved across different species, indicating its evolutionary significance.

# Induction of ER stress in human islets upregulates expression of *SEC* genes

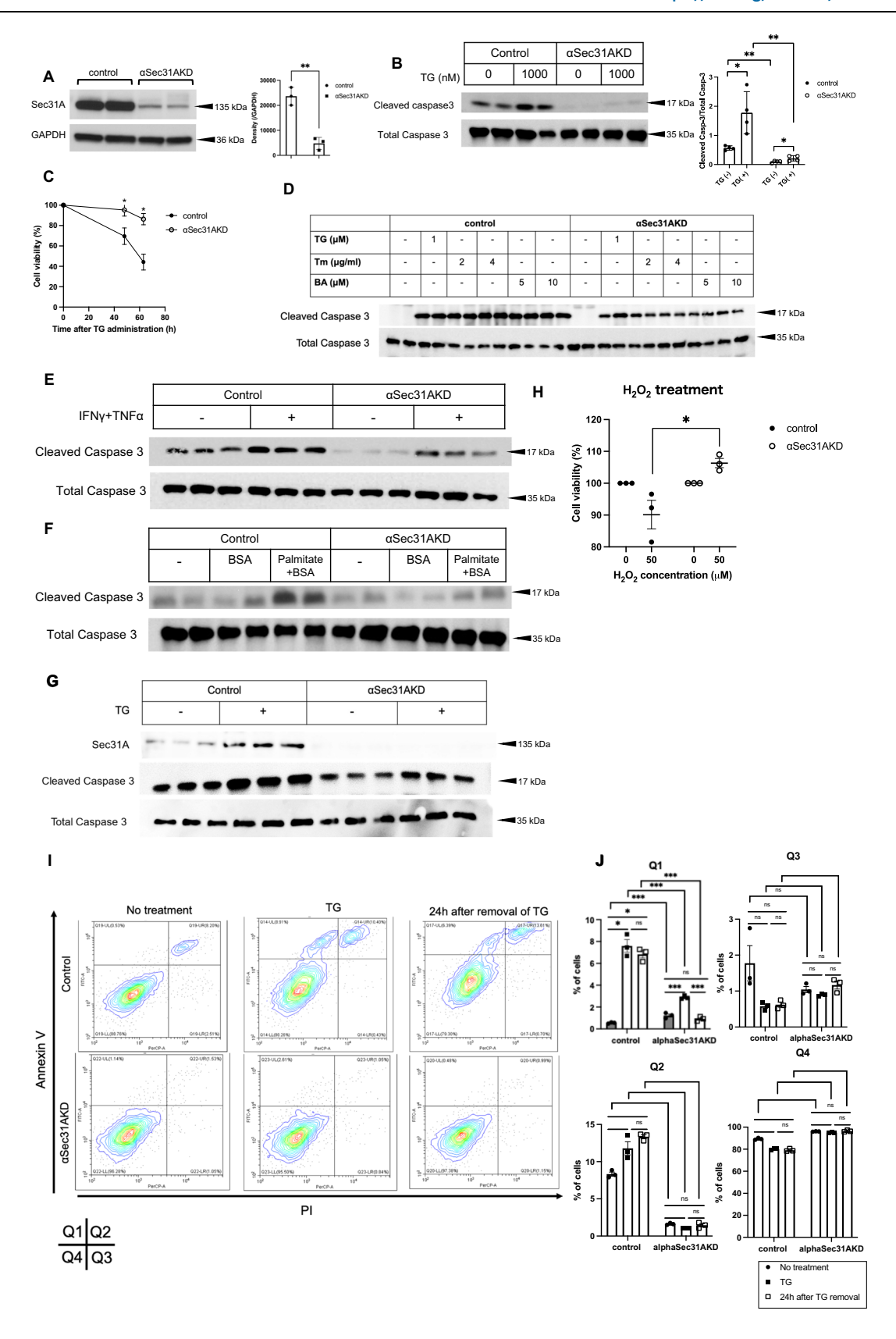
We explored the transcriptional changes induced by ER stress by treating freshly isolated islets from non-diabetic (non-DM) or T1D donors with thapsigargin (TG) for 24 h, followed by RNA-seq analysis (Fig. 4A). First, immunostaining to confirm alpha cell enrichment revealed a predominance of alpha cells in all three T1D islet preparations (Supplementary Fig. 2A). Next, upon induction of ER stress, we observed upregulation in multiple genes related to ER stress and/or apoptosis, such as *DDIT3* (CHOP), *HSPA5* (BiP), *TRIB3*<sup>41</sup>, *HERPUD1*<sup>42</sup>, and *ASNS*<sup>43</sup>, both in non-DM and T1D islets upon TG treatment (Fig. 4B). This validated the successful induction of ER stress. Building on this, we also observed upregulation of *SEC* family genes in both non-DM and T1D islets following TG treatment (Supplementary Fig. 2B). Given that T1D islets are predominantly populated by alpha cells due to the decrease of beta cells, these findings suggest that significant transcriptional changes intensifying both stress-related and *SEC* family gene expression in response to ER stress emanate mostly from alpha cells of T1D islets.

# ER Stress induced expression of SEC genes is mitigated in type 1 diabetes islets

Given that T1D islets are primarily composed of alpha cells and display more pronounced elevation in expression of SEC family genes under ER stress compared to non-diabetic conditions, we further explored the ability of mitigating ER stress on the expression of SEC family genes. To this end, we treated islets with TG, taurodeoxycolic acid (TUDCA), an ER stress mitigator, or a combination of both TG and TUDCA (Fig. 4A, E). We identified distinct differentially expressed genes (DEGs) across the individual treatment groups (Fig. 4E and Supplementary Fig. 2C-E). In a dot plot comparing various pathways related to ER stress, we observed that several pathways upregulated by TG were diminished when it was combined with TUDCA (asterisks in Fig. 4F). This observation was corroborated by a decrease in BiP (Binding Immunoglobulin Protein, an ER stress marker) expression levels in T1D alpha cells following treatment with TG+TUDCA, as assessed by immunohistochemistry (IHC)(Supplementary Fig. 2F). Turning attention to SEC genes, including SEC31A, their expression was increased by TG and diminished when TG was combined with TUDCA (Fig. 4G, H). These results demonstrate that the expression of SEC31A, along with multiple ER stress-related genes and pathways in T1D islets, influenced by external stressors, can be mitigated through the mitigation of ER stress. These results prompted us to investigate the specific pathways impacted by SEC31A in both human alpha and beta cells.

# Distinct alterations in SEC31A expression in alpha and beta cells under stress

To investigate the differences in *SEC31A* expression under stress between human alpha and beta cells, we compared the expression and functional roles of *SEC31A* in both cell types by IHC. For this, non-diabetic human islets were treated with high glucose, IFN-gamma, TNF-alpha, or IL-beta and IFN-gamma, followed by evaluation of *SEC31A* expression in alpha and beta cells. Notably, under normal conditions, *SEC31A* expression was higher in alpha cells compared to beta cells (Fig. 4I, J). Treatment with high glucose and cytokines led to a significant upregulation of *SEC31A* expression in alpha cells, while the increase observed in beta cells was comparatively modest (Fig. 4J).



These results suggest that *SEC31A* plays a relatively distinct role in alpha cells compared to beta cells in responding to high glucose- and cytokine-induced stress. Related to these results, we also extracted expression data for *SEC31A* from a recently published paper on multiplexed single-cell RNA sequencing<sup>44</sup>. This was used to define the

transcriptional signature of primary human islet cells exposed to the ER stressor Brefeldin A, *SEC31A* exhibited a higher fold increase in alpha cells compared to beta cells, which supports the hypothesis that alpha cells have a distinct response to ER stress (Supplementary Fig. 2G).

#### Fig. 2 | AlphaSec31AKD cells show survival phenotype against ER stress.

A Generation of alphaSec31A KD cells. Left: Immunoblots of control cells and alphaSec31A cells. Quantification is shown in the right panel. Data are presented as mean values  $\pm$  SEM. (two-tailed Student's t test). \*\*p < 0.01. Three biological replicates cultured in independent wells were examined. **B** Immunoblots of control and  $\alpha$ Sec31A knockdown cells treated with thapsigargin (TG, 1  $\mu$ M) for 5 h. Quantified band intensities are presented as mean  $\pm$  SEM. One-way ANOVA revealed a significant overall difference among groups (p = 0.0001), and Tukey's post-hoc test was used to assess pairwise significance.\*p < 0.05, \*\*p < 0.01. Four biological replicates cultured in independent wells were examined. **C** Cell viability assays of control and alphaSec31A cells. n = 6 (0 h, 48 h), n = 4 (63 h), each representing an independent biological replicate. Data are presented as mean values  $\pm$  SEM. (two-tailed Student's t test). \*p < 0.05. **D** Immunoblots of cleaved caspase-3 after treating control and alphaSec31A cells with thapsigargin (TG), tunicamycin (Tm), and Brefeldin A (BA) for

5 h. Figure **E**, **F** Immunoblots of control and αSec31A cells treated with TNFα (1000 U/ml) and IFN-γ (1000 U/ml) (**E**) or palmitate (500 μM) for 16 h (**F**). **G** Immunoblots of control and siRNA-mediated Sec31A knockdown cells treated with TG (1 μM) for 5 h. **H** Cell viability of control and αSec31A KD cells after concentration-dependent  $H_2O_2$  treatment (n=3, each an independent biological replicate). Data are presented as mean values  $\pm$  SEM. (two-tailed Student's t test). \*p < 0.05. **I**, **J** Flow cytometric analysis of apoptosis in control and αSec31A knockdown cells treated with thapsigargin (TG, 1 μM for 5 h) and following 24 h of TG removal (n=3 independent biological replicates). **I** Representative quadrant dot plots (**J**) Quantification of cell populations across quadrants (Q1–Q4) under control, TG, and post-TG recovery conditions. Data are presented as mean  $\pm$  SEM. Two-way ANOVA revealed significant main and/or interaction effects, and Tukey's post-hoc test was applied to assess pairwise differences. \*p < 0.05, \*\*p < 0.01,\*\*\*p < 0.001. Data are presented as mean values  $\pm$  SEM. Source data are provided as a Source Data file.

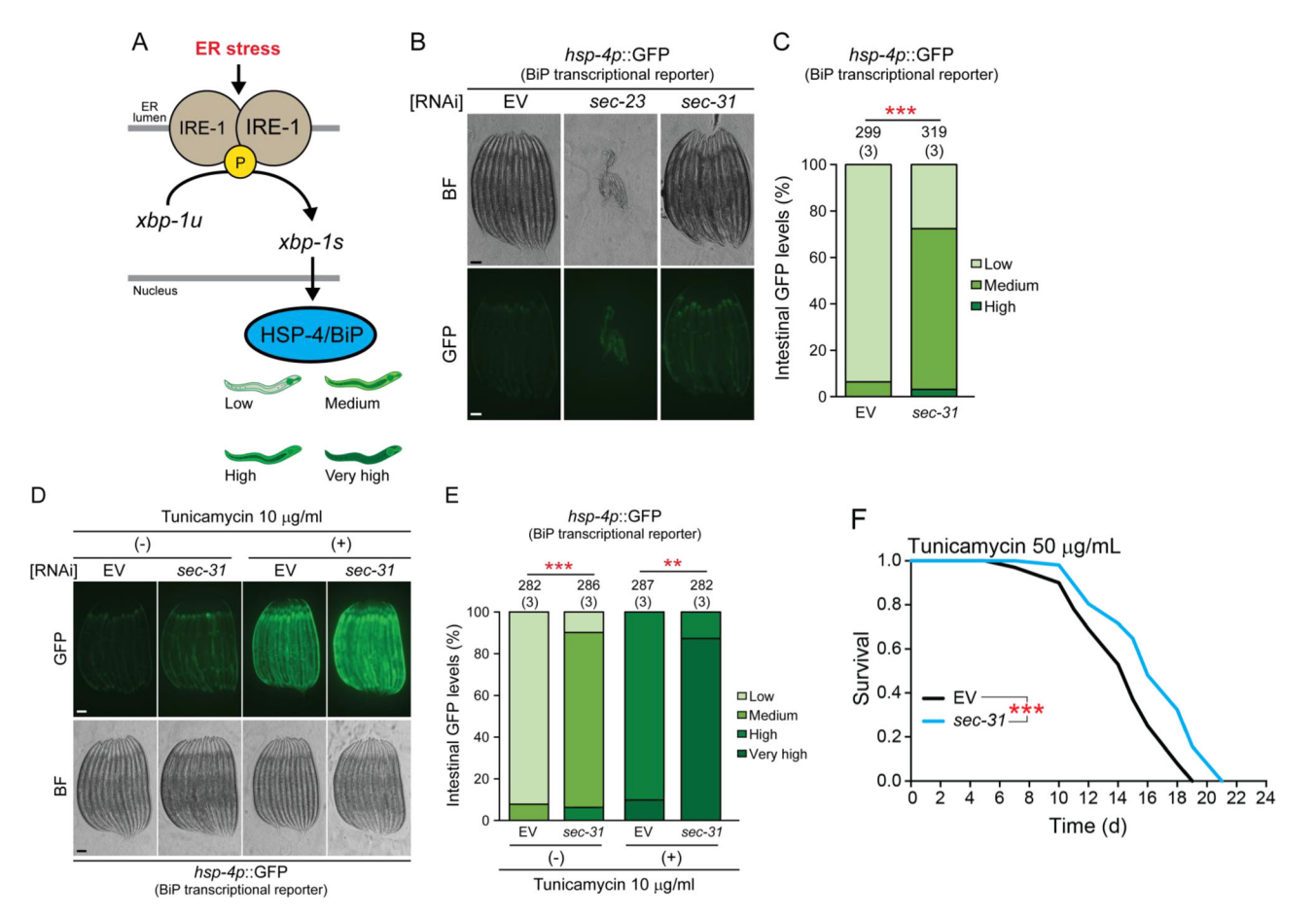


**Fig. 3** | **Sec31A** inhibition induces a protective organismal response against ER stress. **A** UPR<sup>ER</sup> stress response in *C. elegans* assessed by the transcriptional reporter *hsp-4p*::GFP and qualitative quantified by GFP intensity. **B** Bright field (BF) and GFP microscopy images of hsp-4p::GFP worms grown under COPII inhibition by KD of *sec-23* and *sec-31*. Scale bar, 100 µm. **C** Quantification of the *hsp-4* transcriptional response after RNAi against *sec-31* (See Supplementary Data 4 for details). **D** Knockdown of *sec-31* allowed a greater UPR<sup>ER</sup> transcriptional response when subjected to ER stress by tunicamycin. Scale bar, 100 µm. **E** Quantification of

biological replicates shown in **(D)**. Data in **(C, D)** were analyzed using a two-sided Chi-square test to compare the frequency of fluorescent signal distribution between groups. No adjustments were made for multiple comparisons. **F** COPII inhibition by  $\sec 31$  KD allowed greater survival under ER stress conditions (see Supplementary Table 1 for survival details, replicates, and statistics). Numbers above bars denote sample size (biological replicates), \*\*p < 0.01, \*\*\*p < 0.001. Source data are provided as a Source Data file.

We next investigated the effect of Sec31A on hormone production and secretion in both cell types. First, using alphaTC6 cells, we examined glucagon secretion, transcription, and content. While glucose-responsive glucagon secretion is impaired upon TG induction in control cells, alphaSec31AKD cells exhibited enhanced glucagon secretion at low glucose concentrations (1 mM) and did not demonstrate a significant reduction in secretion following TG induction, regardless of the glucose concentration (Supplementary

Fig. 3A). This was consistent with glucagon production, as Sec31AKD alpha cells showed increased glucagon content compared to control cells (Supplementary Fig. 3B). Next, using qPCR, we found TG reduced the expression of glucagon, proglucagon, and PCSK2, while Sec31A deletion in alphaTC6 cells significantly increased their expression (Supplementary Fig. 3C). On the other hand, polysome profiling of the cells to assess global protein translation showed no significant difference between control and alphaSec31AKD cells,

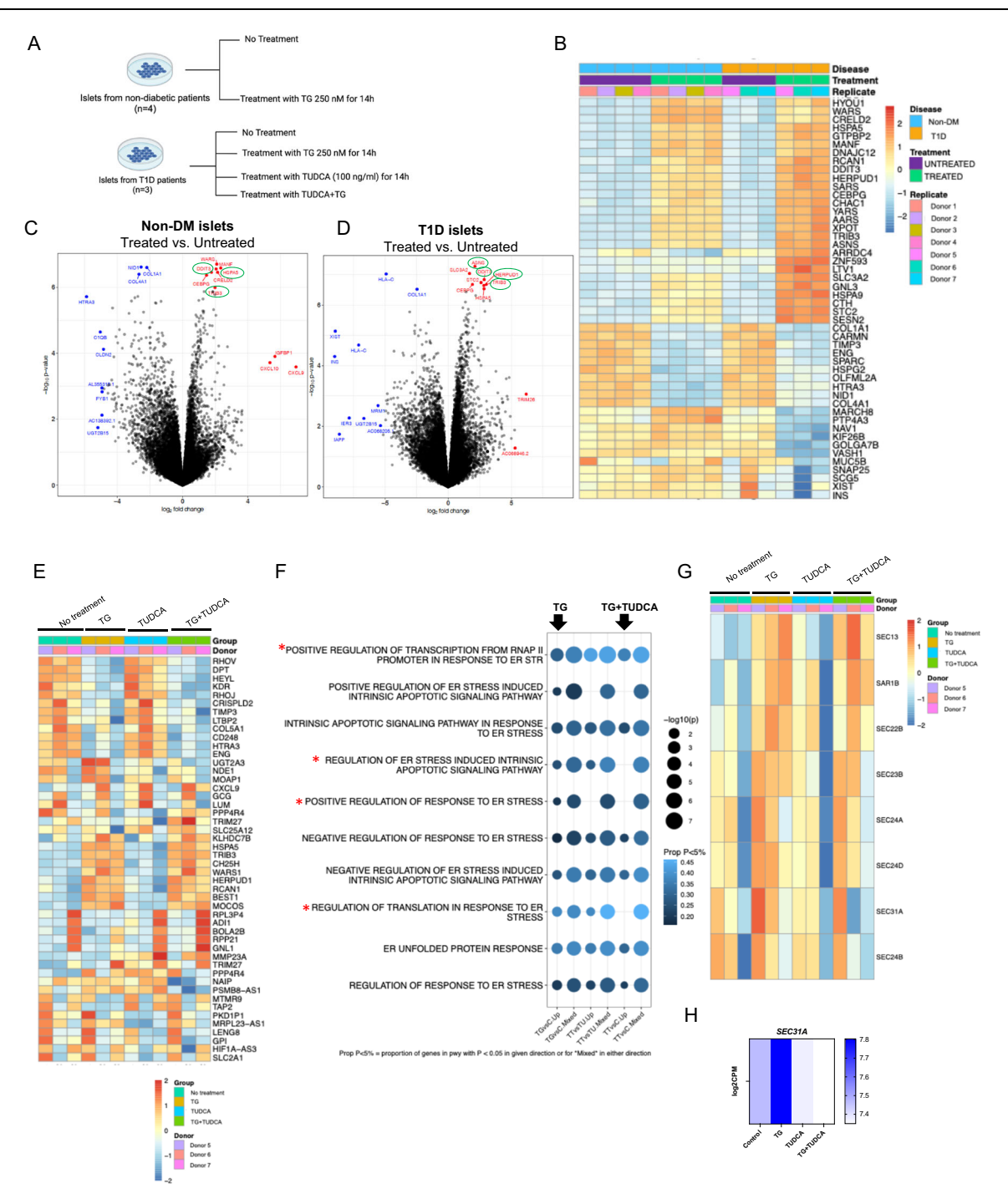


Fig. 4 | Mitigation of SEC Gene Expression Under ER Stress in Type 1 Diabetes Islets. A Human islets sourced from non-diabetic (non-DM) and Type 1 Diabetes (T1D) donors, incubated for 24 h in Miami medium, with or without the addition of thapsigargin (TG) at a concentration of 250 nM. Created in BioRender. Shibue, K. (2025) https://BioRender.com/7w1qe08. B Heatmap representing the log2 (fold change) of the top differentially expressed genes (DEGs) after TG treatment in non-DM and T1D islets, alongside the SEC family genes originally identified in the CRISPR screen (as depicted in Fig. 1). C, D Volcano plot of genes in non-DM (C) and T1D (D) islets treated with TG. Differential gene expression was assessed using limma with moderated two-sided t tests. Equivalence testing for unchanged genes (fold change < 20%) was performed using two one-sided t tests (TOST). P-values were adjusted for multiple comparisons using the Benjamini-Hochberg FDR correction. E Heatmap of T1D islets treated with TG, TUDCA, and their mixture. Donor numbers (5-7) in the figure correspond to those in Fig. 4B and Supplementary Table 2. F Dot plots of ER stress-related pathways in T1D islets treated with TG, TUDCA, and their mixture. Differential expression was analyzed using limma with linear modeling and

moderated two-sided t tests. P-values were adjusted for multiple testing using the Benjamini-Hochberg FDR method. **G** Gene expressions of SEC family genes, including SEC31A, in T1D islets treated with TG, TUDCA, and their mixture. N=3 for T1D, each representing an independent biological replicate. Donor numbers (5–7) correspond to those in Fig. 4B and Supplementary Table 2. **H** SEC31A expression levels expressed as  $\log_2$  CPM under control (no treatment), TG, TUDCA, and TG + TUDCA conditions (blue shading reflects expression level: darker blue = higher expression, lighter blue = lower expression). **I** Immunohistochemistry of non-diabetic human islets treated with media containing TNF $\alpha$  (1000 U/ml), IE-1 $\beta$  (50 U/ml) + IFN $\gamma$ , and 19 mM glucose was stained with antibodies against insulin (INS), glucagon (GCG), and SEC31A. Treatment time was 24 h. N=3, each representing an independent biological replicate. Scale:20  $\mu$ m. For the demographics of donors, see Supplementary Table 2. **J** Quantification of SEC31A-positive cells shown in (**I**). Data is presented as mean values  $\pm$  SEM. (two-tailed Student's t test). \*p < 0.05. Source data are provided as a Source Data file.

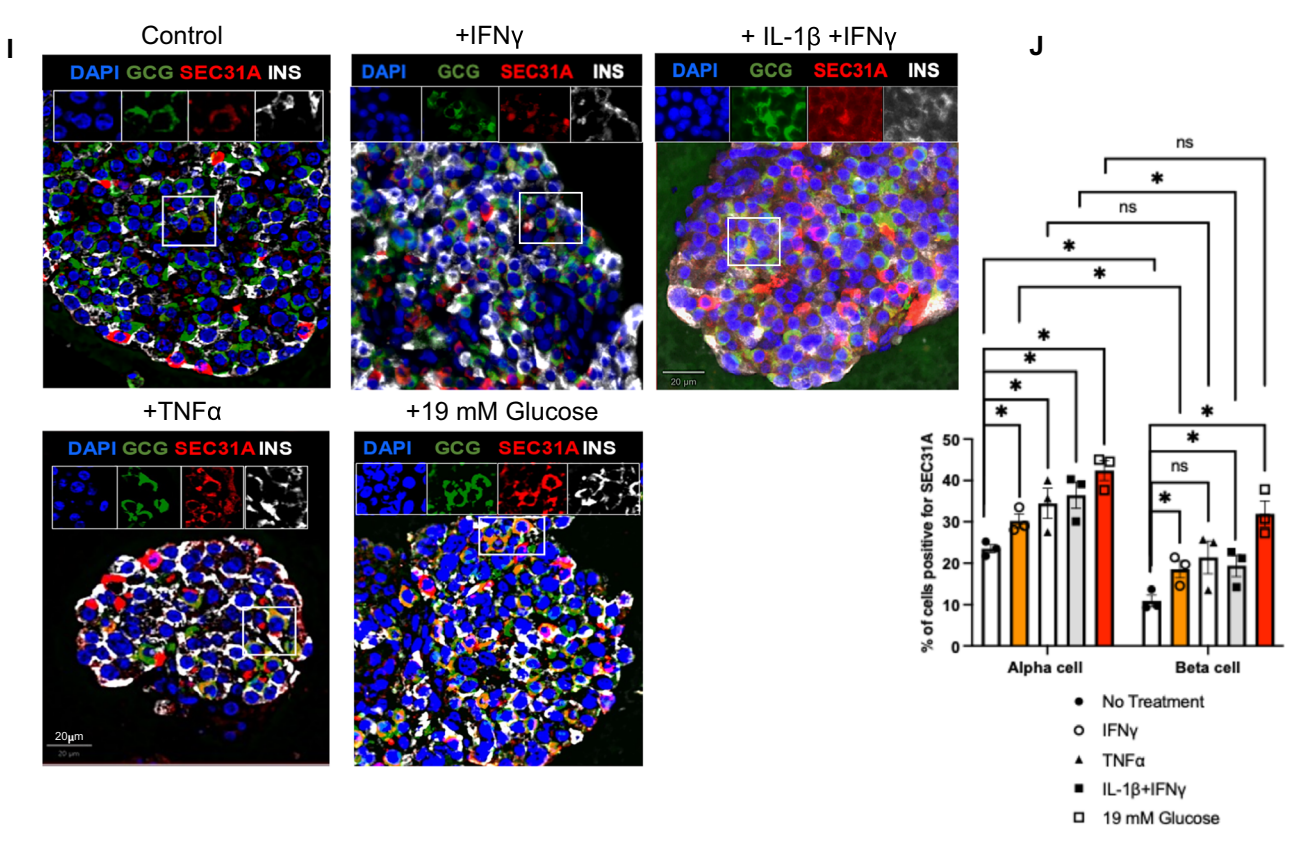


Fig. 4 | Continued.

suggesting that Sec31A is unlikely to underlie global translation (Supplementary Fig. 3D).

To assess the effect of *SEC31A* on insulin secretion and content in beta cells, we used the human-derived EndoC-βH5 cell line which closely mimics primary adult human beta cells<sup>45</sup> since the purity of the beta cells achieved by using DA-ZP1 was between 80 to 85%)<sup>46</sup>. We transfected these cells with human *SEC31A* siRNA on day 3 after seeding (Supplementary Fig. 3E). By day 7, cells showed no morphological changes (Supplementary Fig. 3F), and *SEC31A* knockdown exceeded 70% (Supplementary Fig. 3G). Glucose-stimulated insulin secretion (GSIS) was comparable between control and SEC31AKD beta cells (Supplementary Fig. 3H). However, insulin content was significantly reduced in SEC31AKD beta cells (Supplementary Fig. 3I).

These findings highlight the differential expression and response of *SEC31A* to external stressors in human islets. *SEC31A* appears to have distinct effects on hormone production between alpha and beta cells, affecting glucagon and insulin differently. To further explore the mechanism of decreased insulin content in SEC31AKD beta cells, we performed qPCR to examine the expression of genes responsible for insulin synthesis or secretion. *GCK*, which plays a role in insulin secretion by increasing ATP production during glucose metabolism, is decreased in SEC31AKD cells. Meanwhile, *ABCC8 (SUR1)*, which encodes the regulatory subunit of the ATP-sensitive potassium channel involved in modulating insulin secretion, *KCNJ11* (Kir6.2), an ATP-sensitive potassium channel that triggers insulin secretion and *PCSK1*, which is involved in the processing of proinsulin to insulin, did not show significant changes between the two cell lines (Supplementary Fig. 3J).

# Gene analysis in human pseudoislets reveals differential effects of *SEC31A* knockdown between alpha and beta cells

To gain direct insight into the role of *SEC31A* in human islet cells, we examined genes and pathways in alpha- and beta-pseudoislets generated from human islets. Briefly, human islet cells were sorted using flow cytometry after staining with fluorescein-based compounds. The

fractions of alpha and beta cells were segregated based on a recently established method<sup>46</sup>. The sorted alpha and beta cells were cultured for seven days to generate pseudoislets (Fig. 5A). Consistent with our previous studies<sup>46-48</sup>, the expected purity of INS-positive cells (-85%) and GCG-positive cells (~95%) was achieved, thereby confirming the reliability of the cells used for the experiments. To achieve stable knockdown of SEC31A, we designed lentiviral CRISPR vectors coding gRNA of human SEC31A and confirmed that the SEC31A gene was knocked down (~40%) in the pseudoislets (alpha- or beta-SEC31AKD) (Fig. 5B, C). After lentiviral transduction, the pseudoislets were cultured for 7 days (Fig. 5D, E) and subjected to RNA-seq analyses (Fig. 5F-H). In alphaSEC31AKD cells, the upregulated genes included HSP90AA1, members of the Heat Shock Protein (HSP) family such as HSPA1B, HSP90B1, and HSPD1, and endoplasmic reticulum proteins PDIA3 and CANX. In addition, eukaryotic translation initiation factors EIF3A and EIF4B, along with the cell growth factor MRFAP1, were notably increased (Fig. 5H, I). While betaSEC31AKD cells also exhibited upregulation of HSP90AA1 and EIF4B, similar to alpha cells, they showed increased expression of UBC, P4HB, SEC24D, FN1, and RRAGA, which have all been previously reported to have a functional link to the stress response (Fig. 5H, J). This suggests a common stress response involving HSP90AA1 and EIF4B in both cell types, and also highlights distinct cell type-specific regulatory responses.

Utilizing the GeneMANIA database<sup>49</sup> for prediction of gene function prediction and STRING<sup>50</sup> database for clarifying a functional protein–protein interaction network, we observed central network nodes in alphaSEC31AKD cells involving the Heat Shock Protein family and eukaryotic translation initiation factors. These nodes regulate the unfolded protein response and cell survival<sup>51</sup>. Gene Ontology (GO) term analyses of the differentially expressed genes (DEGs) with a significance of p < 0.001 indicated upregulation of genes related to ER function and ER stress response, including responses to topologically incorrect proteins, protein folding, and ER stress in alphaSEC31AKD cells (Fig. 5K). Meanwhile, the enriched pathways in betaSEC31AKD

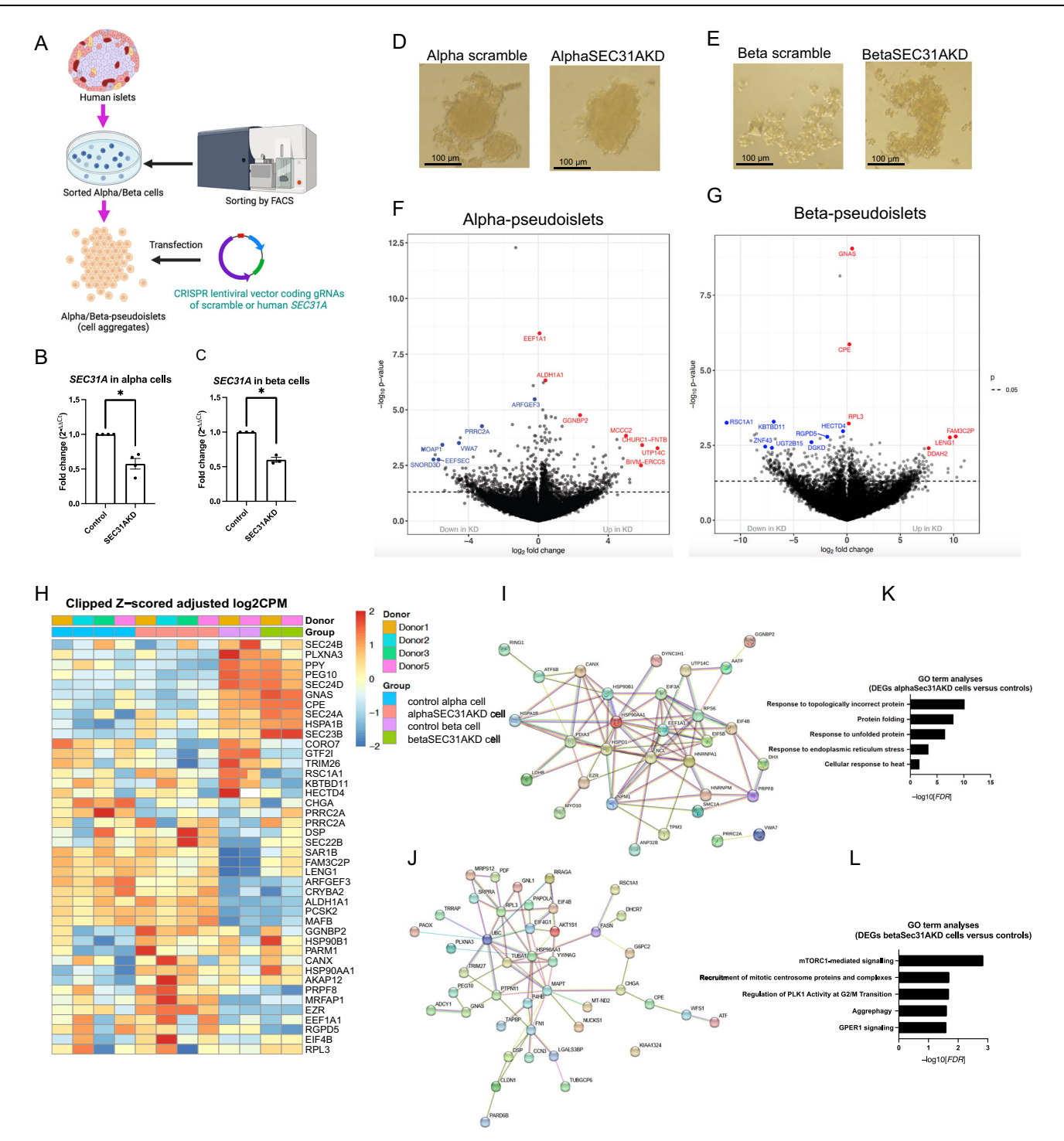
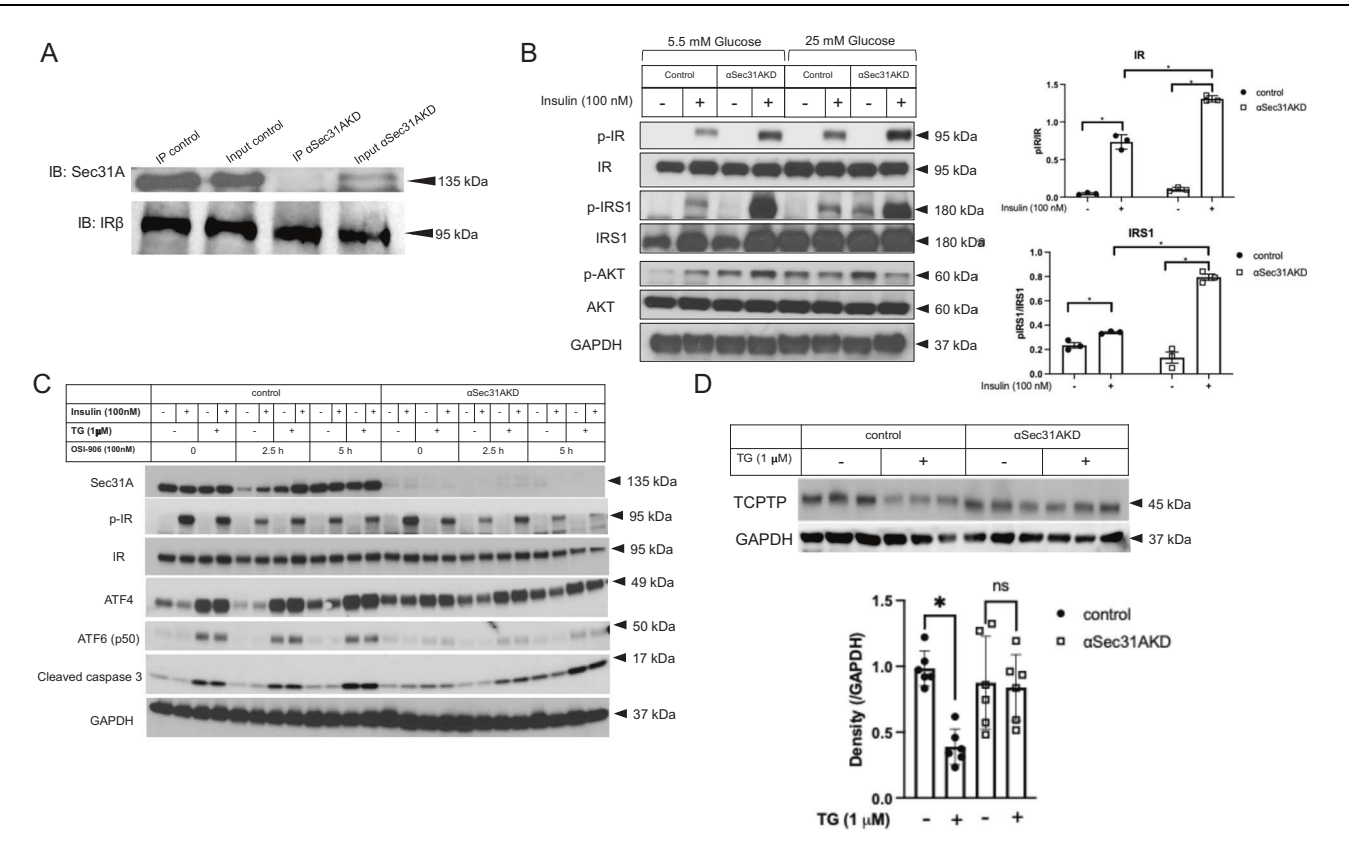


Fig. 5 | Molecular analyses of human islet cells with SEC31A knock down.

**A** Human alpha and beta cells sorted from cadaveric human islets were incubated in Miami media for seven days to generate pseudoislets. Created in BioRender. Shibue, K. (2025) https://BioRender.com/x9b8puh. **B**, **C** qPCR results showing SEC31A expression between control and SEC31AKD alpha (**B**) and beta (**C**) pseudoislets. Biological replicates, n = 4 for alpha cells and n = 3 for beta cells, each representing an independent biological replicate. Data are presented as mean values  $\pm$  SEM. Twotailed Student's t test; \*p < 0.05. **D**, **E** Representative images of control and SEC31AKD alpha pseudoislets (**D**) and beta pseudoislets (**E**). **F**, **G** Volcano plots comparing control and SEC31AKD alpha pseudoislets (**F**) and beta pseudoislets (**G**). Differential expression was analyzed using limma with linear modeling and moderated two-sided t tests, incorporating surrogate variables as covariates. FDR was

controlled using the Benjamini-Hochberg method. **H** Heatmap of selected genes up-regulated in SEC31AKD alpha pseudoislets. Biological replicates, n=4 for alpha cells and n=2 for beta cells, each representing an independent biological replicate. **I**, **J** STRING analysis of the functional protein-protein interaction network of up-regulated genes in SEC31AKD alpha pseudoislets (n=4, each representing an independent biological replicate)(**I**) and beta pseudoislets (n=2, each representing an independent biological replicate)(**J**). **K**, **L** Enriched GO term analyses showing significantly up-regulated genes in SEC31A-KD alpha pseudoislets (n=4, each representing an independent biological replicate) (**K**) and beta pseudoislets (n=2, each representing an independent biological replicate)(**L**). Source data are provided as a Source Data file.



**Fig. 6** | **Sec31A** cross talks with proteins in insulin/IGF1 signaling pathway. **A** Coimmunoprecipitation of IRβ and Sec31A in alphaTC6 cells. Immunoblots of Sec31A in cell lysates that were immunoprecipitated with IRβ and Sec31A. **B** AlphaSe31AKD cells exhibited enhanced phosphorylation of insulin signaling pathways, independent of glucose concentration. Cells were treated with 100 nM insulin for 15 min following overnight starvation in DMEM containing either 5.5 mM or 25 mM glucose. The right panel displays the quantification of p-IR/IR and p-IRS1/IRS1 in the presence of 25 mM glucose. Data are presented as mean values  $\pm$  SEM. (two-tailed Student's t test). \*p < 0.05, \*\*p < 0.01. Three biological replicates cultured in

independent wells were examined. **C** Repression of TG-induced cleaved caspase-3 elevation in alphaSec31A cells was not observed when TG was administered with OSI-906. Immunoblots of cleaved caspase-3 in control and alphaSec31A cells treated with/without TG and OSI-906. **D** Immunoblots of TCPTP in control and alphaSec31A cells after the treatment with TG. Quantification is shown in the lower panel. Data are presented as mean values  $\pm$  SEM. (two-tailed Student's t test). \*p < 0.05. Six biological replicates cultured in independent wells were examined. Source data are provided as a Source Data file.

cells include mTORC1 signaling and the cell cycle, indicating distinct regulatory pathways (Fig. 5L). In addition, there were fewer genes related to the endoplasmic reticulum compared to alphaSEC31AKD cells, underscoring the specific stress response and signaling mechanisms activated in beta cells. These results suggest that SEC31A knockdown leads to alterations in different pathways in alpha and beta cells, particularly in the context of ER stress.

# Deletion of Sec31A facilitates cell-protective effects through interaction with the insulin receptor

To examine the mechanism(s) underlying the stress-resistance phenotype induced by Sec31A inhibition, we considered the observation that Sec31A interacts with insulin receptor beta (IR beta)<sup>52</sup>. Considering that IR is involved in cell growth<sup>53–55</sup>, we began by performing communoprecipitation of alphaTC6 cells to confirm physical binding between IR $\beta$  and Sec31A (Fig. 6A). Next, to elucidate a functional link between Sec31A and IR $\beta$ , we treated control or alphaSec31AKD cells with insulin (100 nM) and examined phosphorylation events in proteins in the insulin signaling pathway. Regardless of the glucose concentration in the media, alphaSec31AKD cells showed increased levels of p-IR and p-IRS1 in response to insulin (Fig. 6B), indicating that a lack of Sec31A in alphaTC6 cells enhances insulin signaling.

To examine the involvement of growth factor signaling in the stress-resistance phenotype, we treated alphaSec31AKD cells with TG in combination with OSI-906, an inhibitor of IR and IGF-1R<sup>56,57</sup>. While induction of cleaved caspase-3 after TG treatment was reproducibly

suppressed in alphaSec31AKD cells, the suppression was not observed when the cells were treated with a combination of TG and OSI-906 (Fig. 6C). This indicates that the blunted inhibition of cleaved caspase-3 noted in alphaSec31AKD cells after TG treatment is dependent on insulin signaling. To investigate the impact of long-term insulin treatment on Sec31A expression and cell survival, we exposed both control and alphaIRKD cells to insulin and thapsigargin (TG) for five hours. Our findings indicate that the absence of insulin receptors in alphaIRKD cells resulted in elevated levels of cleaved caspase-3 upon ER stress induction, suggesting that insulin may contribute to mitigating apoptosis (Supplementary Fig. 4).

Next, we explored the factor(s) potentially mediating the functional link between IR $\beta$  and Sec31A. TCPTP is a key phosphatase that downregulates insulin signaling by dephosphorylating the IR<sup>58,59</sup>. While TG treatment significantly downregulated the expression of TCPTP in control cells, the effect was blunted in alphaSec31A cells (Fig. 6D). Taken together, these findings highlight the important role of Sec31A in regulating TCPTP expression and insulin signaling.

Finally, we compared the impact of *SEC31A* knockdown on insulin signaling pathways in alpha- and beta-pseudoislets (Fig. 5) by analyzing RNA-seq data and calculating z-scores for genes involved in insulin signaling. First, in our transcriptomic analysis of pseudo-islets from alpha- and betaSEC31AKD cells, we re-analyzed the apoptotic gene pathway (Supplementary Fig. 5A, B) and observed that the expression levels of multiple genes in apoptotic pathways differ between alpha- and betaSEC31AKD cells. Within the context of insulin signaling, we

identified several differentially expressed genes related to cell survival, such as *BAD* (BCL2-associated agonist of cell death) (Supplementary Fig. 5C, D). Its activity is modulated by phosphorylation under growth factor stimulation, which reduces its apoptotic function<sup>60,61</sup>. However, these transcriptomic changes alone are insufficient to conclusively establish a causal link between *SEC31A* and cell survival in alpha cells, and further functional studies are necessary to clarify this relationship.

Collectively, these results lay the foundation for future studies aimed at comprehensively elucidating the impact of Sec31A on insulin signaling pathways and its role in ER stress.

# **Discussion**

Patients with diabetes encounter metabolic stress, including ER stress, leading to potential dysfunction and/or death of islet cells<sup>62</sup>. The exposure of islet cells to high levels of glucose, lipids, and inflammation in patients with diabetes (both T1D and T2D) and the consequent altered secretory demand<sup>63</sup> can trigger a stress response to promote cellular dysfunction<sup>64</sup>. Despite its clinical importance, the mechanism(s) that limit the glucagon response to hypoglycemia in compromised pancreatic alpha cells remain poorly understood<sup>65</sup>. In this study, we tested the hypothesis that alpha cells possess an intrinsic stress resistance mechanism by conducting a genome-wide CRISPR screen to identify Sec31A as a potential regulator of cell survival under ER stress<sup>66</sup>.

A genome-wide CRISPR screen is a powerful technique that uses the CRISPR-Cas9 system to systematically knock out or modify genes across the entire genome, enabling the identification of key genes involved in diverse cellular processes, such as cell survival, proliferation, or disease pathways. This method was developed by harnessing CRISPR-Cas9's ability to create targeted gene disruptions, and it has since been adapted for high-throughput functional genomics screening, offering a comprehensive approach to discovering gene function<sup>27,30</sup>. These screens have been applied in various research fields, including identifying novel therapeutic targets and understanding disease mechanisms, such as in diabetes research, where CRISPR screens have helped reveal critical genes for beta-cell protection and survival<sup>35</sup>.

In our study, we employed a negative selection CRISPR screen to uncover genes that shield alphaTC6 cells from ER stress-induced cell death. Unlike positive selection screens, negative selection screens shed light on survival mechanisms, which is essential for our objective to find ways to enhance alpha cell functionality. Previous studies have similarly used negative screens, such as identifying calreticulin as a regulator of ATF6 $\alpha$  signaling under ER stress<sup>67</sup>, and to discover protective glycosylation pathway genes<sup>68</sup>.

A complementary approach is to ensure a more rigorous selection of stress-resistance genes involved using a two-step TG treatment strategy for alpha cells, starting with a lower concentration and escalating up to 250 nM. This concentration was originally chosen based on its proven effectiveness reported by Cai et al. in NIT-1 beta cells<sup>35</sup>, where it clearly differentiated survival outcomes between control and mutant cells under high-stress conditions, making it ideal for robustly assessing ER stress resistance in our context. Furthermore, this concentration was also used in a recent study employing a multi-omics approach to investigate the impact of ER stress on transcriptional regulatory networks in human islets at a genome-wide level<sup>69</sup>. This intense protocol allowed us to distinguish ER stress resistance in alpha cells by subjecting them, alongside beta cells, to sustained ER stress conditions; only alpha cells exhibited resilience under these conditions, thereby highlighting their unique stress-response capacity compared to beta cells.

We found that gRNAs targeting *Sec* gene family members were enriched in the cell population that survived 250 nM TG treatment, demonstrating that the loss of these genes contributes to enhanced cell survival under stress conditions. *Sec* genes are part of the outer layer of COPII and considered to be recruited from the cytosol to the

ER membrane in the COPII formation process<sup>70,71</sup>. For example, a previous study showed that deletion of SEC24A led to cell survival under TG-induced ER stress, highlighting the specific role of SEC24A in facilitating stress-induced cell death<sup>72</sup>. It has also been reported that downregulation of SEC24C in human hepatocellular carcinoma (HCC) suppressed cell proliferation and chemoresistance, indicating that SEC24C interacts with EIF2AK3 (PERK) and activates UPR-related apoptosis<sup>73</sup>. Moreover, a recent report has drawn attention to the absence of Sec31A in regenerating nerve fibers in the skin<sup>74</sup>, providing another example of cell-specific and context-dependent roles of Sec family genes. Our additional analysis regarding the role of Sec31A in stress reversibility indicates that its effect on stress resistance confers a durable improvement in cellular recovery following stress removal. Future studies are warranted to dissect the molecular mechanism(s) by which Sec31A enhances cellular resilience following ER stress induction and removal.

We extended our study to an in vivo model in *C. elegans* with constitutive overexpression of spliced *xbp-1*<sup>38</sup> to induce ER stress. The study indicates that knockout of *sec-31* promotes survival under tunicamycin-induced UPR<sup>ER</sup> and suggests that the *sec-31* null model's cytoprotective phenotype is conserved across species.

The data from RNA-seq analysis of T1D islets in our study provides translational evidence supporting the role of *SEC31A* in stress responses in human islets impacted by T1D. It is important to note that the samples comprise various cell types, although alpha cells are likely to predominate in T1D islets<sup>24</sup>. In addition, it is important to note that our study involved older individuals as non-diabetic subjects compared to those with T1D, which may influence the comparative baseline expression levels of *SEC31A* between the groups.

Further comparative analyses of T1D islets treated with TUDCA or a combination of TG and TUDCA indicate that the upregulation of *SEC31A* expression following TG treatment is subject to mitigation. TUDCA alleviates ER stress, prevents disruptions in the unfolded protein response, and reinforces mitochondrial stability<sup>75</sup>. These findings suggest that *SEC31A* expression adapts to varying stress levels, underscoring its capacity for regulation through external stress management, an important consideration in T1D, where alpha cells experience sustained stress exposure. This opens potential strategies for protecting alpha cells and promoting their recovery by reducing *SEC31A* expression levels, leading to the restoration of alpha cell survival.

To clarify the role of *SEC31A* in alpha and beta cells, we analyzed its expression in response to high glucose and inflammatory cytokines using immunohistochemistry. Our findings show that both cell types utilize *SEC31A* elevation as a common stress response mechanism, although baseline *SEC31A* levels differ. This suggests that while both alpha and beta cells engage similar pathways to manage stress, *SEC31A* likely drives unique downstream effects in each.

In this study, we also examined Sec31A's influence on endocrine secretion from islet cells. Knockdown of Sec31A in alphaTC6 cells increased glucagon release specifically at low glucose concentrations and maintained consistent secretion rates following TG induction. This basal elevation in glucagon corresponded with increased content and transcription levels in these cells. Conversely, such changes were not observed in human-derived EndoC- $\beta$ H5 cells. Although species differences should be taken into consideration to interpret the data, our findings suggest that Sec31A differentially regulates secretory pathways in alpha and beta cells, indicating distinct roles in glucose-regulated secretion. Notably, previous studies on the involvement of Sec31A in hormone secretion are very limited. This highlights the novelty of our findings and underlines the need for further investigation.

Significant differences exist in the distribution and population of alpha cells between rodents and humans<sup>76</sup>, which, along with the limited availability of sorted human alpha cells suitable for culture, has historically hindered the translation of rodent findings to human contexts. To overcome this challenge, our group previously

established a method for harvesting alpha-pseudoislets from human islets<sup>46</sup>. Building on this methodological foundation, our current study expanded the analysis to include both alpha- and beta-pseudoislets. This comprehensive approach allowed us to compare differentially expressed genes (DEGs) across these cell types, identifying genes uniquely influenced by *SEC31A* in human alpha cells, thereby enhancing our understanding of its role in islet biology.

Considering that transfecting primary human cells presents challenges, we achieved a fair reduction in SEC31A mRNA levels by 40%, consistent with outcomes reported in previous studies<sup>77,78</sup>. The resulting phenotype suggests potential haploinsufficiency in our model, as even this modest reduction was sufficient to disrupt alpha cell function and homeostasis. Studies with more complete knockdown may further clarify SEC31A-dependent mechanisms. Evaluation of the upregulated pathways in SEC31A knockdown alpha-pseudoislets showed enrichment of genes encoding Heat Shock Protein 70 (*HSP70*)<sup>79</sup>, *HSP90*<sup>80</sup>. The HSPs have been reported to prevent apoptosis by binding to Apaf, and disrupting the formation of the apoptosome to inhibit the activation of caspase-9 and caspase-381,82. These functional links between SEC31A and HSPs may contribute to the stress-resistant phenotype in alpha cells. Indeed, HSPA1B was upregulated in SEC31A KD alpha pseudoislets (Fig. 5H). Notably, Gaulton et al.83 identified genetic variants near HSPA1B associated with type 1 diabetes (T1D); however, their analysis suggested that the primary effect of these variants is mediated through HLA-DQA1, located in the same genomic region. Thus, although HSPA1B expression changes may be relevant to stress resistance, its direct contribution to T1D susceptibility remains to be clarified.

Growth factor signaling is essential for the survival and growth of various metabolic cell types, including beta cells<sup>84-86</sup>. In the context of hepatic function, a functional interplay between SEC31A and growth factor signaling has been reported. For example, SEC31A has been shown to modulate hepatic lipid metabolism by dissociating from CRTC2 phosphorylation at Ser136 via mTOR regulation, as part of the SREBP1 pathway<sup>87</sup>. In addition, a co-immunoprecipitation analysis in mouse liver identified SEC31A among the most significant IRBassociated peptides<sup>52</sup>. In our study, we observed a similar interaction between SEC31A and IRB in alpha cells, along with increased IR phosphorylation following insulin stimulation. This suggests that SEC31A may play a regulatory role in insulin signaling pathways, which are known to influence alpha cell biology88. Furthermore, our transcriptomic analysis indicates that genes responsible for cell survival and death downstream of the insulin signaling pathway are differentially altered in alpha- and beta-pseudoislets following SEC31A knockdown. While we identified suggestive pathways linking insulin signaling-dependent apoptotic modulation to SEC31A knockdown, further functional analyses focusing on multiple key apoptotic regulators are warranted.

We have noted potential limitations in this study. First, the use of isolated islet cells excludes paracrine effects present in their native state within the islets. This impacts the accuracy of studying cell behavior outside their original microenvironment. For example, previous studies have shown that intra-islet mediators like insulin<sup>88</sup>. somatostatin<sup>89</sup>, and GABA<sup>90</sup> significantly influence alpha cell biology. Our findings on protein transfers between beta and exocrine cells<sup>91</sup> suggest the need to further investigate alpha cell interactions with acinar cells. These issues become relevant given the challenges of contamination by exocrine cells within the islet preparations. Second, our findings are limited by the difficulty of acquiring live T1D islets at different stages of disease progression. In addition to their limited availability, achieving high sample purity remains challenging due to the inevitable inclusion of non-endocrine cells. While this technical constraint may introduce variability, our analysis still offers valuable insights into SEC gene expression under stress conditions in the context of T1D, underscoring the clinical relevance of studying live human islets.

Finally, stress induction using thapsigargin may not fully capture the complex and gradual progression of alpha cell dysfunction that occurs in vivo. These limitations warrant further studies to explore the translational applicability of these findings.

In conclusion, our study identifies Sec31A as a novel regulator of alpha cell survival in response to ER stress. These findings reaffirm the value of genome-wide approaches in studying cellular stress response mechanisms and offer research directions to better understand the pathophysiology of alpha cell dysfunction in diabetes.

# **Methods**

### **Cell Lines**

AlphaTC6 cells were purchased from ATCC (CRL-2934). Beta cell lines derived from male mice were established following the methods outlined in previous studies  $^{92,93}$ . EndoC- $\beta$ H5 (Lot #S-23001), a human beta cell line, was purchased from Human Cell Design (Toulouse, France).

### Generation of lentiviral vector library

We used the mouse Brie pooled CRISPR library (Addgene Cat No.73632), targeting 19,674 genes with 4 gRNAs per gene for CRISPR screen<sup>30</sup>. Transduction by the lentiviral CRISPR library and subsequent screening with thapsigargin (TG) were undertaken as described previously<sup>35</sup>. Briefly, to generate the Brie lentiviral CRISPR library, HEK293T cells were transfected with the Brie CRISPR plasmid library. Polyethylenimine (Sigma No.408727) was used at a dose three times the total transfected DNA in the transfection. Aliquots of the media were collected on days 3 and 4, and virus particles were precipitated using PEG-it Virus Precipitation Solution 5X. Precipitated particles were filtered and stored at – 80 °C until use.

#### Transduction of alphaTC6 Cells with Lentiviral Vector Library

AlphaTC6 cells were incubated with DMEM (10-013-CV, Corning, NY, USA) containing 4.5 g/L glucose and 10% fetal bovine serum. For transduction, the cells were plated 24 h before viral infection and then incubated with lentivirus for 24 h (MOI = 0.3). Selection was done with 4  $\mu$ g/mL of puromycin 48 h after the transduction, and continued for 14 days prior to the experiments.

# Selection of cells by thapsigargin

We prepared a stock solution of TG (1 mM; Santa Cruz Biotechnology; CAS 67526-95-8) by dissolving in DMSO. After the puromycin-selected cells reached confluence, 50 nM of TG was added to the media for the initial selection of cells. After removing TG from the media, we allowed the survived cells to grow to full confluence. Cells were then exposed to ER stress by 100, 150, or 250 nM of TG treatment, respectively. Seven days after treatment, TG was removed from the media and the surviving cell population was grown to confluence.

### **Next-generation sequencing (NGS)**

Genomic DNA from the harvested samples were purified, the DNA fragment flanking the gRNA sequence was amplified and adapter sequences were introduced by PCR. The amplicon library were then sequenced by Illumina next-generation sequencing (NGS) (DNA Link (Seoul, South Korea)). The raw reads of the NGS are presented as log2 expression of gRNA. The sequences of primers used for the PCR are listed in Supplementary Data 3. The SBGNview R package (Luo and Brouwer 2013) was used for the mapping.

#### Data analysis of NGS raw data and pathway analysis

The pathway analyses of the top enriched gRNAs, based on GO terms, were conducted at the Joslin Bioinformatics Core (Boston, MA). The top 50 sgRNAs were systematically selected based on the enrichment of each gRNA, from top 1 to top 50, avoiding arbitrary selection. For the analysis of protein-protein interaction networks, the proteins encoded by these RNAs were examined using STRING, a tool

specifically designed for such analysis. In parallel, Kinase Enrichment Analysis 3 (KEA3) (https://maayanlab.cloud/kea3/), a web-based database, and GeneMANIA database (https://genemania.org/) for prediction of gene function prediction were employed to identify the kinases that phosphorylate the genes of interest.

#### Generation of stable knockdown of Sec31A in alphaTC6 cells

To establish a Sec31A-deficient cell line model, we transfected alphaTC6 cells with mouse Sec31A CRISPR/Cas9 KO plasmid (Santa Cruz Biotechnology, CA, USA, Cat No. sc-427321) and mouse Sec31A HDR plasmid (Santa Cruz Biotechnology, CA, USA, Cat No. sc-427321-HDR) using TurboFectin 8.0 transfection reagent (Origene, DE,USA,Cat No. TF81001). Seventy-two hours after transfection, the cells were selected by adding  $4\,\mu\text{g}/\mu\text{L}$  of puromycin to the culture media. Puromycin-resistant cells were seeded on fresh culture plates, and the cells were serially propagated.

### Cell viability assay

The assay was performed using a Cell Titer Glo luminescence cell viability kit (Promega, Madison, Wisconsin, USA, #7570) according to the manufacturer's instructions. Approximately,  $1\times10^6$  cells were seeded in opaque-walled 96-well plates and  $100~\mu\text{L}$  of Cell Titer Glo reagent was added to each well. The cells were collected at each time point. The contents were mixed for 2 min on an orbital shaker and incubated for 10 min at room temperature. Luminescence was recorded using a Promega GloMax luminometer with an integration time of 0.3 sec per well.

#### Flow cytometry

Flow cytometry was performed as reported previously  $^{91,94}$ . Briefly, cells were resuspended in DMEM with 0.05% of trypsin. Subsequently, the cells were centrifuged, and aliquots of media were removed. Cells were washed with 1X Binding Buffer (BB) and filtered through a 40  $\mu$ m filter. Filtered solution was diluted so that the concentration reached 1 million cells/100  $\mu$ L 1X BB. Next, 100  $\mu$ L of the solution was aliquoted in a 5 mL FACS tube, followed by the addition of 5  $\mu$ L of FITC AnnexinV (#556419, BD Biosciences) and 10  $\mu$ L of propidium iodide (PI) (#81845, Sigma). Cells were incubated for 15 min at RT and analyzed by FACS Aria (Joslin Flow Cytometry Core). The apoptotic cell rate was determined as a percentage of Annexin V-negative/PI-positive (necrotic) and Annexin V-positive cell (apoptotic) populations.

# Worm strains and RNAi treatment

The wild-type N2 strain and *hsp-4p*::GFP line (SJ4005)<sup>40</sup> were maintained on nematode growth medium (NGM) plates seeded with *Escherichia coli* (OP50) at 20 °C using standard techniques (Brenner, 1974). The RNAi method was performed in accordance with the protocol described in the recent study<sup>95</sup>.

# **UPR** transcriptional reporter

The *hsp-4p*::GFP line (SJ4005) was maintained and grown at 20 °C. To assess the effect of KD *sec-3I* RNAi, L1 bleach-synchronized worms were grown on the corresponding EV (HT115) and *sec-3I* dsRNA bacteria. After 48 h, 2.5 mL of either tunicamycin or vehicle (DMSO) was added, and the worms were incubated for 24 h at 20 °C. Worms were quantified under UV light for GFP fluorescence, and images were captured with an Olympus IX51 microscope and cellSens standard 1.12 software. Designation of low, medium, high, or very high categories (Fig. 3A) were based on the GFP intensity and intestine distribution. Raw data are provided in Supplementary Data 4. Chi-square tests were used for statistical analyses.

#### ER stress survival assay

L1 seeded worms in either EV or *sec-31* dsRNA bacteria were transferred to pre-treated tunicamycin plates (2 mL of 50 µg/mL of tunicamycin or

DMSO vehicle until dry, containing FuDR to prevent progeny proliferation) with the appropriate bacterial type. After worms had dispersed in the plate (30 min), 2.5 mL of 50 µg/mL of tunicamycin or DMSO vehicle was added, and survival was scored every day and plotted. Significance was assessed by the log-rank test. Details of survival analyses are provided in Supplementary Table 1.

#### **SDS-PAGE** and Western blotting

Cells were lysed with radioimmunoprecipitation buffer (Thermo Fisher, Waltham, Massachusetts, USA) for Western blotting analysis. The total protein concentration was determined using a bicinchonic acid assay (#23223 and #23224, Thermo Fisher). Samples were resuspended in reducing SDS-PAGE sample buffer, boiled, and resolved by SDS-PAGE. Proteins were subsequently transferred onto polyvinylidene difluoride membranes, treated with blocking buffer (Thermo Scientific), and incubated with primary antibodies overnight at 4 °C. Cleaved Caspase-3 (Asp175) (#9661; Lot 47), GAPDH (#5174; Lot 1), Sec31A (#13466; Lot 1), phospho-Insulin Receptor β (Tyr1345) (#3026; Lot 17), TCPTP (#58935; Lot 1), ATF4 (#11815), ATF6 (#65880), phospho-Akt (Ser473) (#9271), and Akt (#9272) antibodies were purchased from Cell Signaling Technology (Danvers, Massachusetts, USA). The phospho-IRS1 (Tyr896) antibody (Cat. #44-818 G) was purchased from Thermo Fisher Scientific. The IRS-1 antibody (#06-248; Lot 3850453) was purchased from Millipore. All antibodies were used at a 1:1000 dilution.

# Culturing of human type 1 diabetes islets and induction of ER stress

Islets from donors with type 1 diabetes (T1D) following staining with dithizone were kindly provided by A. Powers, MD (Vanderbilt University, Nashville, TN, USA). Written informed consent was obtained from all donors. A total of 100 islets per experimental condition were handpicked and submitted for RNA sequencing. During handpicking, cluster-like structures, suggestive of acinar cells, were excluded. Nondiabetic control islets were purchased from Prodo Inc. or the Integrated Islet Distribution Program (IIDP). Clinical information on the pancreatic donors is presented in Supplementary Table 2. All human islets used in this study were obtained in accordance with applicable ethical guidelines and privacy regulations. For islets obtained from Prodo Inc. and IIDP, appropriate informed consent was secured from donors or their legal representatives prior to tissue recovery. All donor information was de-identified before distribution. No identifying information or indirect identifiers that could reasonably lead to donor identification are included in this study. Sex and/or gender of the donors has been retained in accordance with the journal policy on sex and gender reporting.

For the induction of ER stress and its recovery, we treated non-diabetic (non-DM) human islets with or without thapsigargin (TG) (250 nM), and T1D islets with either TG, tauroursodeoxycholic acid (TUDCA) (100 ng/ml), or a mixture of the two. The islets were treated for 24 h before being harvested for RNA-seq.

#### Sorting of alpha and beta cells from human islets using DA-ZP1

Human pancreatic islet cells were enriched for alpha cells using the protocol reported previously<sup>46–48</sup>. Briefly, healthy human pancreatic islets were handpicked, washed with DPBS, and dispersed into single cells by incubating islets in TrypLE (Gibco) for 12–15 min at 37 °C, mixing every 2-3 min. Islet cells were then washed with DMEM containing 15% FBS and resuspended in Miami medium containing 0.03 μM DA-ZP1 and incubated at 37 °C for 20 min. DA-ZP1-treated islet cells were sorted using a FACS Aria cell sorter (BD Biosciences) to remove DA-ZP1+ cells (β cells) from the cell suspension. Enriched alpha cells were centrifuged at  $200 \times g$  for 5 min, and the cell pellet was resuspended in fresh Miami medium with a final cell concentration of 40,000 cells/mL. The cells were dispensed into U-bottom 96-well

plates (8000 cells/200 µL/well) and incubated for one day before lentiviral transduction.

#### Lentiviral transduction of sorted human islet cells

Lentiviral vector carrying human SEC31A guideRNA-Cas9 and scramble vector coding mCherry were purchased from Vector Builder Inc. (Chicago, IL, USA). Enriched alpha and beta cells were transduced with lentiviral particles (2.84  $\times\,10^7$  TU/8000 cells/well) in 30  $\mu$ L of Miami medium containing 10  $\mu$ g/mL polybrene (Sigma). Fresh Miami medium (170  $\mu$ L) was added to the wells 4 to 6 h after transduction, and cells were cultured for 7 days before harvesting.

# GSIS in EndoC-βH5 with SEC31A Knockdown

EndoC- $\beta$ H5 cells were seeded and cultured according to the vendor's protocols. The glucose-stimulated insulin secretion (GSIS) test was conducted following the provided protocol. Briefly, 100  $\mu$ L of  $\beta$ COAT® Coating Matrix aliquots were coated onto 24-well plates and incubated at 37 °C overnight. On Day 0, the thawed cells were seeded at approximately 187,500 cells per well in ULTI $\beta$ 1 Complete culture medium (Human Cell Design). Five hours later, the transfection media was aspirated and replaced with 1X ULTI $\beta$ 1 media.

On Day 3, transfection with siRNA targeting SEC31A was performed. We used 1.5  $\mu L$  of siRNA (scramble: #sc-37007 or SEC31A: #sc-36868, Santa Cruz Biotechnology, USA) and 1.5  $\mu L$  of transfection reagent (#sc-29528, Santa Cruz Biotechnology, USA) mixed into 20.83  $\mu L$  of siRNA Transfection Medium (#sc-36868, Santa Cruz Biotechnology, USA) per well. After 5 h of treatment, the mixture was removed and replaced with 1X ULTIβ1 media. On Day 6, the cells were serum-starved using ULT1-ST® medium. On Day 7, the cells were washed and then incubated in  $\beta KREBS$  buffer (Human Cell Design) supplemented with BSA for 1 h, followed by replacement with new  $\beta KREBS$  buffer containing BSA and either 0 mM or 20 mM glucose. After a 40 min incubation, the aliquots were collected, and the cells were harvested. Insulin levels were measured using a Human Insulin ELISA Kit (Mercodia, Uppsala, Sweden).

### Real-time qPCR

RNA was extracted from cells using NucleoSpin RNA (Takara, Japan), and total RNA was utilized for reverse transcription using ReverTra Ace qPCR RT Master Mix (TOYOBO, Japan). The resulting cDNA was analyzed and amplified using the ABI 7900HT system (Applied Biosystems). ACTB served as the internal control. Primers used were as follows: for human SEC31A, forward: CAGGTGGACAAGAACTCTTGGC and reverse: GACTCAACAATCTCTTTCCAGTTC; for human ACTB, forward: CACCATTGGCAATGAGCGGTTC and reverse: AGGTCTTTGCGGATGTCCACGT. For mouse Sec31A, forward: TGAACAGAGTGCCGAAGAAGA and reverse: TGGTGACGTAATGGGAACAGG, mouse beta actin: GTTACCAACTGGGACGACA, GGGGTGTTGAAGGTCTCAAA.

# siRNA Transfection

One day prior to transfection, alpha TC6 cells were seeded at a density of  $0.5 \times 10^6$  cells per well in a 12-well plate. The siRNA transfection was performed according to the vendor's protocol. Briefly, in separate tubes,  $5\,\mu\text{L}$  of  $5\,\mu\text{M}$  siRNA was mixed with  $95\,\mu\text{L}$  of Opti-MEM<sup>TM</sup> Reduced Serum Medium (#31985062, Thermo Fisher, MA, USA) (Tube 1), and  $5\,\mu\text{L}$  of DharmaFECT Transfection Reagent (#T-2001-01, Horizon Discovery Group plc, Cambridge, United Kingdom) was mixed with  $95\,\mu\text{L}$  of Opti-MEM<sup>TM</sup> Reduced Serum Medium (Tube 2). Both tubes were incubated at room temperature for  $5\,\text{min}$ . After incubation, the contents of Tube 1 and Tube 2 were combined, mixed thoroughly, and incubated at room temperature for 20 min. The entire mixture was then added to  $800\,\mu\text{L}$  of DMEM media with  $10\%\,\text{FBS}$ , antibiotic-free medium, making a total volume of  $1000\,\mu\text{L}$  per well. The cells were incubated with the transfection media for 24 hs, after which the media was replaced with normal growth media. The cells were harvested after

5 days for protein extraction. The siRNAs used were as follows: ON-TARGETplus Non-targeting Pool, 5 nmol (#D-001810-10-05, Horizon Discovery Group plc) and ON-TARGETplus Mouse Sec31a siRNA - SMARTpool, 5 nmol (#L-052447-01-0005, Horizon Discovery Group plc). The siRNAs were resuspended using 5 x siRNA Buffer (#B-002000-UB-100, Horizon Discovery Group plc).

#### Polysome profiling

After incubation of the cells with 100 µg/mL cycloheximide (CHX) (#01810, Sigma-Aldrich, Burlington, Massachusetts, USA) for 10 min at 37 °C, cells were washed in ice-cold PBS containing CHX (50 µg/ml) and lysed in 300 µl polysome buffer [200 mM KCl, 20 mM TrisHCl (pH 7.4), 10 mM MgCl<sub>2</sub>, 1%Triton-X, 50 µ/ml RNasin,100 µg/mL CHX]. The cell lysates were passed through a 25-gauge needle and incubated on ice for 10 min followed by centrifugation at 13,000 × g for 10 min at 4 °C. Supernatant was layered onto a 10–50% sucrose gradient solution containing 20 mM Tris-HCl (pH 7.4), 10 mM MgCl<sub>2</sub>, 200 mM KCl, and 50 µg/ml CHX. The sucrose gradients were subjected to centrifugation at 4 °C in a Beckman SW-41Ti rotor at 39,000 rpm for 2 h. A piston gradient fractionator (BioComp Instruments, Fredericton, Canada) was used to fractionate the gradients, and the absorbance of RNA at 254 nm was recorded using an online UV monitor.

# Lentiviral mediated silencing of insulin receptor

Lentiviral vectors containing shRNA targeting the mouse insulin receptor (IR) and a control non-targeting shRNA were acquired from Open Biosystems. To produce lentivirus, we adhered to the guidelines provided by Open Biosystems. alphaTC6 cells were seeded one day prior to infection and subsequently exposed to the lentivirus for a 24 h period. To establish stable cell lines, selection with puromycin at a concentration of 4 mg/mL commenced 48 h post-infection and continued for - 2 weeks prior to conducting experiments. This process was repeated to create three independent stable cell lines for each group.

# Human islets and cell treatments for immunohistochemistry

Human islets were cultured overnight in Miami media containing 19 mM glucose. The islets were treated for 24 h with either vehicle (PBS), 19 mM glucose, IFN- $\gamma$  (1000 U/ml; Peprotech), IL-1 $\beta$  (50 U/ml; R&D Systems, USA), or TNF- $\alpha$  (1000 U/ml; R&D Systems, Catalog Number: 210-TA-020). The concentrations of cytokines were determined according to previous studies<sup>96,97</sup>. After treatment, the islets were manually selected and washed twice with ice-cold DPBS (GIBCO). For immunofluorescence studies, samples were fixed and embedded in agar using previously described methods<sup>98</sup>. Imaging of human islets was performed using QuPath, an open-source software platform developed for comprehensive bioimage analysis (QuPath, GNU General Public License). The analysis involved positive cell counting for each color channel–DAPI (blue), FITC for glucagon (GCG, green), TRITC for SEC31A (red), and for insulin (INS, white). The results were quantified to determine the percentage of cells positive for SEC31A.

# Statistical analysis

All data are expressed as means  $\pm$  SEM. Statistical analyses were performed using unpaired two-tailed Student's t tests, one-way or two-way ANOVA, followed by appropriate post hoc tests. For multiple comparisons versus a single control group, Dunnett's test was applied using the multcomp package in R, with adjusted p-values based on the single-step method. Differences were considered statistically significant at p < 0.05.

#### Statistics and reproducibility

All experiments were performed with at least three biologically independent replicates unless otherwise specified. For immunohistochemistry, representative images were selected from a minimum of three independent experiments yielding similar results. Quantitative data (e.g., qPCR, Western blot, cell viability assays) were obtained from three or more independent experiments, and data are presented as mean ± SEM unless stated otherwise. For high-throughput analyses (e.g., RNA-seq, CRISPR screen), independent biological replicates were used as detailed in the corresponding figure legends. No statistical methods were used to predetermine sample size. All attempts at replication were successful unless noted otherwise.

#### **Ethics statement**

This study complies with all relevant ethical regulations. The use of human pancreatic islets was approved by the Institutional Review Board of the Joslin Diabetes Center. Human islets were obtained from the Integrated Islet Distribution Program (IIDP), Prodo Laboratories, Inc., and Vanderbilt University, with appropriate informed consent and ethical approval secured by the respective source institutions at the time of donor tissue collection.

### Reporting summary

Further information on research design is available in the Nature Portfolio Reporting Summary linked to this article.

# Data availability

The RNA-seq data of T1D islets and non-diabetic (non-DM) subjects have been deposited in the Gene Expression Omnibus under accession number GSE171352. Similarly, the RNA-seq data of T1D islets treated with thapsigargin (TG) and tauroursodeoxycholic acid (TUDCA) are available under accession number GSE275138. In addition, RNA-seq data from human pseudoislets are available under accession number GSE222009. All other data are contained within this manuscript. All data supporting the findings described in this manuscript are also available from the corresponding author upon request. Source data are provided in this paper.

#### References

- ElSayed, N. A. et al. 2. Classification and diagnosis of diabetes: standards of care in diabetes-2023. *Diabetes Care* 46, S19–S40 (2023).
- Reno, C. M. et al. Severe hypoglycemia-induced sudden death is mediated by both cardiac arrhythmias and seizures. Am. J. Physiol.Endocrinol. Metab. 315, E240–E249 (2018).
- Hitt, T. A. et al. The impact of fear of hypoglycaemia on sleep in adolescents with type 1 diabetes. *Diabet. Med.* 40, e15066 (2023).
- Hædersdal, S., Andersen, A., Knop, F. K. & Vilsbøll, T. Revisiting the role of glucagon in health, diabetes mellitus and other metabolic diseases. *Nat. Rev. Endocrinol.* 19, 321–335 (2023).
- Omar-Hmeadi, M., Lund, P.-E., Gandasi, N. R., Tengholm, A. & Barg, S. Paracrine control of α-cell glucagon exocytosis is compromised in human type-2 diabetes. *Nat. Commun.* 11, 1896 (2020).
- Guo, K., Tian, Q., Yang, L. & Zhou, Z. The role of glucagon in glycemic variability in type 1 diabetes: a narrative review. *Diabetes Metab. Syndr. Obes.* 14, 4865–4873 (2021).
- Hædersdal, S., Lund, A., Knop, F. K. & Vilsbøll, T. The role of glucagon in the pathophysiology and treatment of type 2 diabetes. Mayo Clin. Proc. 93, 217–239 (2018).
- Gromada, J., Chabosseau, P. & Rutter, G. A. The α-cell in diabetes mellitus. Nat. Rev. Endocrinol. 14, 694–704 (2018).
- Braakman, I. & Bulleid, N. J. Protein folding and modification in the mammalian endoplasmic reticulum. *Annu. Rev. Biochem.* 80, 71–99 (2011).
- Sano, R. & Reed, J. C. ER stress-induced cell death mechanisms. Biochim. Biophys. Acta 1833, 3460–3470 (2013).
- Brissova, M. et al. α Cell Function and gene expression are compromised in type 1 diabetes. Cell Rep. 22, 2667–2676 (2018).
- Eisenbarth, G. S. Type I diabetes mellitus. A chronic autoimmune disease. N. Engl. J. Med. 314, 1360–1368 (1986).

- Mezza, T. et al. β-Cell fate in human insulin resistance and type 2 diabetes: a perspective on islet plasticity. *Diabetes* 68, 1121–1129 (2019).
- 14. Cinti, F. et al. Evidence of βcell dedifferentiation in human type 2 diabetes. *J. Clin. Endocrinol. Metab.* **101**, 1044–1054 (2016).
- Inaishi, J. et al. Effects of obesity and diabetes on α- and β-cell mass in surgically resected human pancreas. J. Clin. Endocrinol. Metab. 101, 2874–2882 (2016).
- Marroqui, L. et al. Pancreatic α cells are resistant to metabolic stress-induced apoptosis in type 2 diabetes. EBioMedicine 2, 378–385 (2015).
- Prentki, M., Peyot, M.-L., Masiello, P. & Madiraju, S. R. M. Nutrientinduced metabolic stress, adaptation, detoxification, and toxicity in the pancreatic β-cell. *Diabetes* 69, 279–290 (2020).
- Tersey, S. A. et al. Islet β-cell endoplasmic reticulum stress precedes the onset of type 1 diabetes in the nonobese diabetic mouse model. *Diabetes* 61, 818–827 (2012).
- Clark, A. L. & Urano, F. Endoplasmic reticulum stress in beta cells and autoimmune diabetes. Curr. Opin. Immunol. 43, 60–66 (2016).
- Halban, P. A. et al. β-cell failure in type 2 diabetes: postulated mechanisms and prospects for prevention and treatment. *Diabetes Care* 37, 1751–1758 (2014).
- 21. Kreutzberger, A. J. B. et al. Distinct insulin granule subpopulations implicated in the secretory pathology of diabetes types 1 and 2. *Elife* **9**, e62506 (2020).
- 22. Perez-Serna, A. A., Guzman-Llorens, D., Dos Santos, R. S. & Marroqui, L. Bcl-2 and Bcl-xL in diabetes: Contributions to endocrine pancreas viability and function. *Biomedicines* **13**, 223 (2025).
- Szymczak, F. et al. Transcription and splicing regulation by NLRC5 shape the interferon response in human pancreatic β cells. Sci. Adv. 8, eabn5732 (2022).
- 24. Eizirik, D. L., Szymczak, F. & Mallone, R. Why does the immune system destroy pancreatic  $\beta$ -cells but not  $\alpha$ -cells in type 1 diabetes? *Nat. Rev. Endocrinol.* **19**, 425–434 (2023).
- 25. De Jesus, D. F. et al. Redox regulation of m6A methyltransferase METTL3 in  $\beta$ -cells controls the innate immune response in type 1 diabetes. *Nat. Cell Biol.* **26**, 421–437 (2024).
- Shi, Z. Q. et al. Glucagon response to hypoglycemia is improved by insulin-independent restoration of normoglycemia in diabetic rats. *Endocrinology* 137, 3193–3199 (1996).
- Shalem, O., Sanjana, N. E. & Zhang, F. High-throughput functional genomics using CRISPR-Cas9. *Nat. Rev. Genet.* 16, 299–311 (2015).
- Shalem, O. et al. Genome-scale CRISPR-Cas9 knockout screening in human cells. PLOS Genet. 4, e9 (2008).
- Joung, J. et al. Genome-scale CRISPR-Cas9 knockout and transcriptional activation screening. *Nat. Protoc.* 12, 828–863 (2017).
- Doench, J. G. et al. Optimized sgRNA design to maximize activity and minimize off-target effects of CRISPR-Cas9. *Nat. Biotechnol.* 34, 184–191 (2016).
- 31. Spaeth, J. M. et al. The FOXP1, FOXP2 and FOXP4 transcription factors are required for islet alpha cell proliferation and function in mice. *Diabetologia* **58**, 1836–1844 (2015).
- 32. Heddad Masson, M. et al. Foxa1 and Foxa2 regulate  $\alpha$ -cell differentiation, glucagon biosynthesis, and secretion. *Endocrinology* **155**, 3781–3792 (2014).
- 33. Kanai, M. et al. Genetic analysis of quantitative traits in the Japanese population links cell types to complex human diseases. *Nat. Genet.* **50**, 390–400 (2018).
- 34. Scott, R. A. et al. An expanded genome-wide association study of type 2 diabetes in europeans. *Diabetes* **66**, 2888–2902 (2017).
- 35. Cai, E. P. et al. Genome-scale in vivo CRISPR screen identifies RNLS as a target for beta cell protection in type 1 diabetes. *Nat. Metab.* **2**, 934–945 (2020).

- Henis-Korenblit, S. et al. Insulin/IGF-1 signaling mutants reprogram ER stress response regulators to promote longevity. Proc. Natl. Acad. Sci. USA 107, 9730–9735 (2010).
- Glover-Cutter, K. M., Lin, S. & Blackwell, T. K. Integration of the unfolded protein and oxidative stress responses through SKN-1/Nrf. PLoS Genet. 9, e1003701 (2013).
- 38. Taylor, R. C. & Dillin, A. XBP-1 is a cell-nonautonomous regulator of stress resistance and longevity. *Cell* **153**, 1435–1447 (2013).
- 39. Murphy, C. T. & Hu, P. J. WormBook (2013).
- Calfon, M. et al. IRE1 couples endoplasmic reticulum load to secretory capacity by processing the XBP-1 mRNA. *Nature* 415, 92–96 (2002).
- Fang, N. et al. TRIB3 alters endoplasmic reticulum stress-induced βcell apoptosis via the NF-κB pathway. *Metabolism* 63, 822–830 (2014).
- 42. Ho, D. V. & Chan, J. Y. Induction of Herpud1 expression by ER stress is regulated by Nrf1. FEBS Lett. **589**, 615–620 (2015).
- Gjymishka, A., Su, N. & Kilberg, M. S. Transcriptional induction of the human asparagine synthetase gene during the unfolded protein response does not require the ATF6 and IRE1/XBP1 arms of the pathway. *Biochem. J.* 417, 695–703 (2009).
- 44. Maestas, M. M. et al. Identification of unique cell type responses in pancreatic islets to stress. *Nat. Commun.* **15**, 1–17 (2024).
- Blanchi, B. et al. EndoC-βH5 cells are storable and ready-to-use human pancreatic beta cells with physiological insulin secretion. *Mol. Metab.* 76, 101772 (2023).
- 46. Kahraman, S. et al. Fluorescein-based sensors to purify human  $\alpha$ -cells for functional and transcriptomic analyses. *Elife* **12**, e85056 (2023).
- Lee, M. et al. Native zinc catalyzes selective and traceless release of small molecules in β-cells. J. Am. Chem. Soc. 142, 6477–6482 (2020).
- Kahraman, S. et al. Harnessing reaction-based probes to preferentially target pancreatic β-cells and β-like cells. *Life Sci. Alliance* https://doi.org/10.26508/lsa.202000840 (2021).
- Mostafavi, S. & Morris, Q. Combining many interaction networks to predict gene function and analyze gene lists. *Proteomics* 12, 1687–1696 (2012).
- von Mering, C. et al. STRING: known and predicted protein-protein associations, integrated and transferred across organisms. *Nucleic Acids Res.* 33, D433–D437 (2005).
- Shahbazian, D. et al. Control of cell survival and proliferation by mammalian eukaryotic initiation factor 4B. Mol. Cell. Biol. 30, 1478–1485 (2010).
- 52. Hancock, M. L. et al. Insulin receptor associates with promoters genome-wide and regulates gene expression. *Cell* **177**, 722–736 (2019).
- Shirakawa, J., De Jesus, D. F. & Kulkarni, R. N. Exploring inter-organ crosstalk to uncover mechanisms that regulate β-cell function and mass. Eur. J. Clin. Nutr. 71, 896–903 (2017).
- Okada, T. et al. Insulin receptors in β-cells are critical for islet compensatory growth response to insulin resistance. *Proc. Natl. Acad. Sci. USA* 104, 8977–8982 (2007).
- 55. Folli, F. et al. Altered insulin receptor signaling and β-cell cycle dynamics in type 2 diabetes mellitus. *PLoS ONE* **6**, e28050 (2011).
- Shirakawa, J. et al. Effects of the antitumor drug OSI-906, a dual inhibitor of IGF-1 receptor and insulin receptor, on the glycemic control, β-cell functions, and β-cell proliferation in male mice. Endocrinology 155, 2102–2111 (2014).
- 57. Mezza, T. et al. Nuclear export of FoxO1 is associated with ERK signaling in  $\beta$ -cells lacking insulin receptors. *J. Biol. Chem.* **291**, 21485–21495 (2016).
- Tiganis, T. PTP1B and TCPTP-nonredundant phosphatases in insulin signaling and glucose homeostasis. FEBS J. 280, 445–458 (2013).
- Galic, S. et al. Regulation of insulin receptor signaling by the protein tyrosine phosphatase TCPTP. Mol. Cell. Biol. 23, 2096–2108 (2003).

- Datta, S. R. et al. Akt phosphorylation of BAD couples survival signals to the cell-intrinsic death machinery. Cell 91, 231–241 (1997).
- Zha, J., Harada, H., Yang, E., Jockel, J. & Korsmeyer, S. J. Serine phosphorylation of death agonist BAD in response to survival factor results in binding to 14-3-3 not BCL-X(L). Cell 87, 619–628 (1996).
- Hudish, L. I., Reusch, J. E. B. & Sussel, L. β Cell dysfunction during progression of metabolic syndrome to type 2 diabetes. *J. Clin. Invest.* 129, 4001–4008 (2019).
- Teodoro, J. S., Nunes, S., Rolo, A. P., Reis, F. & Palmeira, C. M. Therapeutic options targeting oxidative stress, mitochondrial dysfunction and inflammation to hinder the progression of vascular complications of diabetes. *Front. Physiol.* 9, 1857 (2018).
- 64. Mukherjee, N., Lin, L., Contreras, C. J. & Templin, A. T. β-Cell death in diabetes: past discoveries, present understanding, and potential future advances. *Metabolites* **11**, 231 (2021).
- 65. Panzer, J. K. & Caicedo, A. Targeting the pancreatic α-cell to prevent hypoglycemia in type 1 diabetes. *Diabetes* **70**, 2721–2732 (2021).
- 66. Bock, C. et al. High-content CRISPR screening. *Nat. Rev. Methods Prim.* **2**, 1–23 (2022).
- Tung, J. et al. A genome-wide CRISPR/Cas9 screen identifies calreticulin as a selective repressor of ATF6α. Elife 13, RP96979 (2024).
- 68. Dalton, H. M. et al. A genome-wide CRISPR screen identifies DPM1 as a modifier of DPAGT1 deficiency and ER stress. *PLoS Genet.* **18**, e1010430 (2022).
- Sokolowski, E. K. et al. Multi-omic human pancreatic islet endoplasmic reticulum and cytokine stress response mapping provides type 2 diabetes genetic insights. Cell Metab. 36, 2468–2488 (2024).
- Crawford, S. E., Criglar, J. M., Liu, Z., Broughman, J. R. & Estes, M. K. COPII Vesicle transport is required for rotavirus NSP4 interaction with the autophagy protein LC3 II and trafficking to viroplasms. *J. Virol.* 94, e01341–19 (2019).
- Koreishi, M., Yu, S., Oda, M., Honjo, Y. & Satoh, A. CK2 phosphorylates Sec31 and regulates ER-To-Golgi trafficking. PLoS ONE 8, e54382 (2013).
- Chidawanyika, T., Sergison, E., Cole, M., Mark, K. & Supattapone, S. SEC24A identified as an essential mediator of thapsigargin-induced cell death in a genome-wide CRISPR/Cas9 screen. Cell Death Discov. 4. 115 (2018).
- Tao, X. et al. SEC24C suppresses the propagation and chemoresistance of hepatocellular carcinoma by promoting unfolded protein response-related apoptosis. *Biosci. Trends* 18, 343–355 (2024).
- Kan, H.-W. et al. Nonpermissive skin environment impairs nerve regeneration in diabetes via Sec31a. Ann. Neurol. 91, 821–833 (2022).
- Vang, S., Longley, K., Steer, C. J. & Low, W. C. The unexpected uses of Urso- and tauroursodeoxycholic acid in the treatment of non-liver diseases. *Glob. Adv. Health Med.* 3, 58–69 (2014).
- 76. Steiner, D. J., Kim, A., Miller, K. & Hara, M. Pancreatic islet plasticity: interspecies comparison of islet architecture and composition. *Islets* **2**, 135–145 (2010).
- 77. Carrillo-Jimenez, A. et al. Effective knockdown of gene expression in primary microglia with siRNA and magnetic nanoparticles without cell death or inflammation. Front. Cell. Neurosci. 12, 313 (2018).
- Lin, Y. et al. Knockdown of PKM2 suppresses tumor progression in human cervical cancer by modulating epithelial-mesenchymal transition via Wnt/β-catenin signaling. Cancer Manag. Res. 10, 4191–4202 (2018).
- Cadena Sandoval, M. et al. mTORC1 Crosstalk With Stress Granules in Aging and Age-Related Diseases. Front. Aging 2, 761333 (2021).
- Dutta Gupta, S., Bommaka, M. K. & Banerjee, A. Inhibiting proteinprotein interactions of Hsp90 as a novel approach for targeting cancer. *Eur. J. Med. Chem.* 178, 48–63 (2019).
- Gober, M. D., Wales, S. Q. & Aurelian, L. Herpes simplex virus type 2 encodes a heat shock protein homologue with apoptosis regulatory functions. Front. Biosci. 10, 2788–2803 (2005).

- Lanneau, D. et al. Heat shock proteins: essential proteins for apoptosis regulation. J. Cell. Mol. Med. 12, 743–761 (2008).
- 83. Chiou, J. et al. Interpreting type 1 diabetes risk with genetics and single-cell epigenomics. *Nature* **594**, 398–402 (2021).
- 84. Kitamura, T. et al. Preserved pancreatic beta-cell development and function in mice lacking the insulin receptor-related receptor. *Mol. Cell. Biol.* **21**, 5624–5630 (2001).
- Kido, Y. et al. Effects of mutations in the insulin-like growth factor signaling system on embryonic pancreas development and betacell compensation to insulin resistance. J. Biol. Chem. 277, 36740–36747 (2002).
- 86. Ueki, K. et al. Total insulin and IGF-I resistance in pancreatic beta cells causes overt diabetes. *Nat. Genet.* **38**, 583–588 (2006).
- Han, J. et al. The CREB coactivator CRTC2 controls hepatic lipid metabolism by regulating SREBP1. Nature 524, 243–246 (2015).
- 88. Kawamori, D. et al. Insulin signaling in alpha cells modulates glucagon secretion in vivo. *Cell Metab.* **9**, 350–361 (2009).
- 89. Rutter, G. A. Regulating glucagon secretion: somatostatin in the spotlight. *Diabetes* **58**, 299–301 (2009).
- 90. Wendt, A. et al. Glucose inhibition of glucagon secretion from rat alpha-cells is mediated by GABA released from neighboring betacells. *Diabetes* **53**, 1038–1045 (2004).
- Kahraman, S. et al. Abnormal exocrine-endocrine cell cross-talk promotes β-cell dysfunction and loss in MODY8. *Nat. Metab.* 4, 76–89 (2022).
- Assmann, A., Ueki, K., Winnay, J. N., Kadowaki, T. & Kulkarni, R. N. Glucose effects on beta-cell growth and survival require activation of insulin receptors and insulin receptor substrate 2. Mol. Cell. Biol. 29, 3219–3228 (2009).
- 93. Kulkarni, R. N. et al. Tissue-specific knockout of the insulin receptor in pancreatic beta cells creates an insulin secretory defect similar to that in type 2 diabetes. *Cell* **96**, 329–339 (1999).
- 94. Shirakawa, J. et al. Insulin signaling regulates the FoxM1/PLK1/ CENP-A pathway to promote adaptive pancreatic β cell proliferation. Cell Metab. **25**, 868–882 (2017).
- Castillo-Quan, J. I. et al. An antisteatosis response regulated by oleic acid through lipid droplet-mediated ERAD enhancement. Sci. Adv. 9, eadc8917 (2023).
- Eizirik, D. L. & Mandrup-Poulsen, T. A choice of death-the signaltransduction of immune-mediated beta-cell apoptosis. *Diabetolo*gia 44, 2115–2133 (2001).
- Delaney, C. A., Pavlovic, D., Hoorens, A., Pipeleers, D. G. & Eizirik, D. L. Cytokines induce deoxyribonucleic acid strand breaks and apoptosis in human pancreatic islet cells. *Endocrinology* 138, 2610–2614 (1997).
- 98. El Ouaamari, A. et al. SerpinB1 Promotes Pancreatic  $\beta$  Cell Proliferation. *Cell Metab.* **23**, 194–205 (2016).

# **Acknowledgements**

The authors thank Alvin Powers, MD (Vanderbilt University, Nashville), for providing human islets from T1D. We also thank Joslin Bioinformatics Core for analyzing RNA-seq data, and the Integrated Islet Distribution Program for providing human islets (NIH Grant # 2UC4DK098085). The authors extend their gratitude to Nobuya Inagaki, MD, PhD, for his substantial support and mentorship to the first author in conducting the research activities necessary for this study. Lastly, we dedicate this work to the memory of T.Keith Blackwell, MD, PhD, in appreciation of his invaluable contributions and support throughout this study. This work is

supported by NIH Grant R01 DK067536 (R.N.K.), the MSD Life Science Foundation and Grant-in-Aid for Young Scientists (K.S.), JSPS KAKENHI (Grant Number JP22K16404) (K.S.), Kitano Cadet-Doctor program 2021-2024 (K.S.), NIH R35GM122610 and R01AG054215 (T.K.B.).

#### **Author contributions**

K.S. conceived the idea, designed, and performed the experiments, analyzed the data and wrote the manuscript. D.D., J.H., J.C., J.H., and H.M. performed the experiments and analyzed the data. P.Y., S.K., and J.H. contributed to planning research designs, data analyses, and conceptual discussions. J.C. and T.K.B. established the worm model and contributed to all the experiments and data analyses using *C.elegans*. R.N.K. contributed to conceiving the study, designing the experiments, discussions, supervising the project and writing the manuscript. All the authors reviewed, commented on and edited the manuscript.

# **Competing interests**

R.N.K. serves on the Scientific Advisory Boards of Novo Nordisk, Biomea and REDD Pharmaceuticals. The other authors declare no competing interests.

### **Additional information**

**Supplementary information** The online version contains supplementary material available at https://doi.org/10.1038/s41467-025-64169-5.

**Correspondence** and requests for materials should be addressed to Rohit N. Kulkarni.

**Peer review information** *Nature Communications* thanks the anonymous, reviewer(s) for their contribution to the peer review of this work. A peer review file is available.

**Reprints and permissions information** is available at http://www.nature.com/reprints

**Publisher's note** Springer Nature remains neutral with regard to jurisdictional claims in published maps and institutional affiliations.

Open Access This article is licensed under a Creative Commons Attribution-NonCommercial-NoDerivatives 4.0 International License, which permits any non-commercial use, sharing, distribution and reproduction in any medium or format, as long as you give appropriate credit to the original author(s) and the source, provide a link to the Creative Commons licence, and indicate if you modified the licensed material. You do not have permission under this licence to share adapted material derived from this article or parts of it. The images or other third party material in this article are included in the article's Creative Commons licence, unless indicated otherwise in a credit line to the material. If material is not included in the article's Creative Commons licence and your intended use is not permitted by statutory regulation or exceeds the permitted use, you will need to obtain permission directly from the copyright holder. To view a copy of this licence, visit <a href="https://creativecommons.org/licenses/by-nc-nd/4.0/">https://creativecommons.org/licenses/by-nc-nd/4.0/</a>.

© The Author(s) 2025